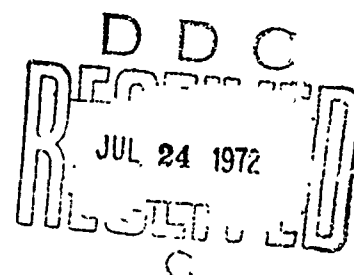


AD 745344

NOLTR 72-15

EXPLOSIVE BEHAVIOR OF ALUMINIZED  
AMMONIUM PERCHLORATE

By  
Donna Price  
A. R. Clairmont, Jr.  
J. O. Erkman



2 MAY 1972

NOL

NAVAL ORDNANCE LABORATORY, WHITE OAK, SILVER SPRING, MARYLAND

NOLTR 72-15

APPROVED FOR PUBLIC RELEASE;  
DISTRIBUTION UNLIMITED

NATIONAL TECHNICAL  
INFORMATION SERVICE

83  
7

UNCLASSIFIED

Security Classification

DOCUMENT CONTROL DATA - R & D

Security classification of title, body of abstract and indexing annotation must be entered when the overall report is classified

1. ORIGINATING ACTIVITY (Corporate author) <b>Naval Ordnance Laboratory White Oak, Silver Spring Maryland 20910</b>		2a. REPORT SECURITY CLASSIFICATION <b>UNCLASSIFIED</b>	
		2b. GROUP	
3. REPORT TITLE  <b>EXPLOSIVE BEHAVIOR OF ALUMINIZED AMMONIUM PERCHLORATE</b>			
4. DESCRIPTIVE NOTES (Type of report and inclusive dates)			
5. AUTHOR(S) (First name, middle initial, last name)  <b>DONNA PRICE, A. R. CLAIRMONT, Jr., and J. O. ERMAN</b>			
6. REPORT DATE <b>2 May 1972</b>		7a. TOTAL NO OF PAGES <b>86</b>	7b. NO OF REFS <b>16</b>
8a. CONTRACT OR GRANT NO		9a. ORIGINATOR'S REPORT NUMBER(S)  <b>NOLTR 72-15</b>	
b. PROJECT NO <b>MAT-03L-000/ROLL-01-01</b>			
c. <b>ORD-033-102-F009-06-01</b>		9b. OTHER REPORT NO(S) (Any other numbers that may be assigned this report)	
d.			
10. DISTRIBUTION STATEMENT  <b>Approved for public release; distribution unlimited.</b>			
11. SUPPLEMENTARY NOTES		12. SPONSORING MILITARY ACTIVITY <b>Naval Material Command Naval Ordnance Systems Command Washington, D. C. 20360</b>	
13. ABSTRACT <p>Addition of aluminum to ammonium perchlorate (AP) increases its infinite diameter detonation velocity, decreases its critical diameter and (at sufficiently low % TMD) the Eyring reaction zone length. For 7-9% AP and 7% Al, the maximum of these effects occurred at about 10% Al. Regular detonation behavior could be observed only in the range of 55 to 40 (or lower) % TMD. All mixtures tested in this range exhibited group 2 behavior as does AP itself.</p> <p>Details of illustrations in this document may be better studied on microfiche</p> <p><i>1a</i></p>			

UNCLASSIFIED

Security Classification

KEY WORDS	LINK A		LINK B		LINK C	
	ROLE	WT	ROLE	WT	ROLE	WT
Detonation velocity						
Ammonium perchlorate						
Aluminized Ammonium Perchlorate						
Composite Propellant Model						

IL

**UNCLASSIFIED**  
Security Classification

EXPLOSIVE BEHAVIOR OF ALUMINIZED AMMONIUM PERCHLORATE

Prepared by

Donna Price, A. R. Clairmont, Jr., and J. O. Erkman

ABSTRACT: Addition of aluminum to ammonium perchlorate (AP) increases its infinite diameter detonation velocity, decreases its critical diameter and (at sufficiently low % TMD) the Eyring reaction zone length. For 7-9 $\mu$  AP and 7 $\mu$  Al, the maximum of these effects occurred at about 10% Al. Regular detonation behavior could be observed only in the range of 55 to 40 (or lower) % TMD. All mixtures tested in this range exhibited group 2 behavior as does AP itself.

Approved by:

CARL BOYARS, Chief  
Advanced Chemistry Division  
Chemistry Research Department  
NAVAL ORDNANCE LABORATORY  
Silver Spring, Maryland 20910


NOLTR 72-15

2 May 1972

EXPLOSIVE BEHAVIOR OF ALUMINIZED AMMONIUM PERCHLORATE

This work was carried out under the tasks MAT-03L-000/R011-01-01, FR 159 and ORDTASK 033-102-F009-06-01 which has now been terminated. It was part of a continuing program on the systematic investigation of the explosive behavior of composite propellant models. The results of this research improve our understanding of the detonation hazards of solid propellants.

ROBERT WILLIAMSON II  
Captain, USN  
Commander

  
ALBERT LIGHTBODY  
By direction

## CONTENTS

	Page
INTRODUCTION .....	1
EXPERIMENTAL .....	2
Materials .....	2
Charge Preparation and Experimental Procedure .....	3
RESULTS AND DISCUSSION .....	6
Detonation Velocity Behavior .....	6
AP/Al, 95/5 .....	6
General Relations for $D(\Delta, u)$ .....	11
AP/Al, 90/10 .....	15
AP/, 80/20 .....	21
Comparison of $D(\Delta, u)$ for AP/Al with that of other composite explosives .....	25
Effect of Al on $D_i$ .....	29
Detonability and Shock Sensitivity .....	32
Chemical Considerations .....	35
Prediction of D .....	37
Eyring Reaction Zone Length .....	44
SUMMARY .....	46
REFERENCES .....	48
APPENDIX A   Dry Blending of Mixtures Containing AP .....	A-1
APPENDIX B   Information on $D = D(\Delta, u)$ for Aluminized Organic H.E. ....	B-1
APPENDIX C   Aluminized Organic H.E. at Constant Diameter .....	C-1

ILLUSTRATIONS

Figure	Title	Page
1	Typical Streak Record. Shot 893 of AP/Al, 95/Al, 95/5, at $\rho_0 = 1.087$ g/cc .....	5
2	Effect of Charge Density and Diameter on Detonation Velocity of AP/Al, 95/5 .....	9
3	Extrapolation to Infinite Diameter Detonation Velocity of AP/Al, 95/5, Data (a. $\Delta = 0.4047$ , b. $\Delta = 0.5498$ ) .....	10
4	Variation of Coefficients of D vs $\Delta$ Curves for AP/Al, 95/5, with Reciprocal Diameter .....	13
5	Effect of Charge Density and Diameter on Detonation Velocity of AP/Al, 90/10 .....	17
6	Extrapolation of Smoothed Data of AP/Al, 90/10, to Infinite Diameter Detonation Velocity .....	18
7	Variation of Coefficients of D vs $\Delta$ Curves for AP/Al, 90/10, with Reciprocal Diameter .....	20
8	Effect of Particle Size of AP and Al on Detonation Velocity of AP/Al, 90/10 .....	23
9	Explosive Group 2 Behavior of AP/Al, 90/10 .....	26
10	Explosive Group 1 Behavior of TNT/Al, 67.8/32.2 ....	27
11	Explosive Group 2 Behavior of AP/Wax, 80/20 .....	28
12	Effect of Al on $D_i$ of AP (a. D vs $\Delta$ Curves, b. $D_i$ and Relative Rate vs % Al).....	30
13	Effect of Aluminum on Detonation Velocity (d = 51 mm) of TNT. (a. D vs $\Delta$ curves, b. D and Relative Rate vs % Al) .....	31
14	Detonability of AP/Al Mixtures .....	34
15	Effect of Aluminum on Detonation Velocity of AP ...	42
A1.a.	Charge ( $\rho_0 = 1$ g/cc) Prepared from Coarest Fraction of Tumbled AP. Shot 720. ....	A-3
A1.b.	9 $\mu$ AP/5 $\mu$ Al, 90/10, Routine Mixing, $\rho_0 = 1.28$ g/cc. Shot 614.....	A-3
A2	AP( $\sim 7\mu$ )/Al( $\sim 5\mu$ ), 90/10, Prepared in Waring Blender with Plastic Beads .....	A-6
A3	AP( $\sim 7\mu$ )/Al( $\sim 5\mu$ ), 90/10, Prepared in Twin Shell Blender .....	A-6
A4	AP( $\sim 7\mu$ )/Al( $\sim 5\mu$ ), 90/10, Prepared in Twin Shell Blender with Ceramic Balls .....	A-8
A5	Charge Pressed from 90/10 Mix of 25 $\mu$ AP/25 $\mu$ Al in Paint Mixer with Porcelain Balls .....	A-8
A6	Charge Pressed from 90/10 Mix of 7 $\mu$ AP/5 $\mu$ Al in Paint Mixer with Porcelain Balls .....	A-9

## ILLUSTRATIONS

Figure		Page
A7	Three Component Propellant Model Mixed in Twin Shell Blender with Four Golf Balls .....	A-9
A8	Three Component Mix prepared in the Twin Shell Mixer with Ceramic Balls .....	A-11
B1	Variation of Coefficients a(u), b(u) for HBX-1 ...	B-5
B2	Variation of Coefficients a(u), b(u) for Tritonal 67.8/32.2 .....	B-6
C1	Variation of Coefficients a, b with Aluminum Concentration.....	C-3

## TABLES

Table	Title	Page
1	Detonation Velocity Measurements on AP/Al, 95/5 .....	7
2	Coefficients for Linear Portion of D vs $\Delta$ Curves of AP/Al, 95/5 .....	12
3	Detonation Velocity Measurements on AP/Al, 90/10, ( $\rho_v = 2.006$ , AP-141, 7.2 ) .....	16
4	Coefficients for Linear Portion of D vs $\Delta$ Curves for AP/Al, 90/10 .....	19
5	Effect of Particle Size on Detonation Velocity of AP/Al Mixtures .....	22
6	Detonation Velocity Measurements on AP/Al, 80/20, ( $\rho_v = 2.065$ g/cc) .....	24
7	Gap Test Results on AP-144/Al-H5, 95/5 .....	33
8	Computed Parameters for Deflagration of AP/Al, 90/10 .....	38
9	Comparison of Ratios Computed from EQ(22) with Experimental Values (Aluminized Organic H.E.) ....	40
10	Comparison of Ratios Computed from EQ(22) with Experimental Values (Aluminized AP) .....	41
11	Effect of Aluminum on Eyring Reaction Zone Length of AP .....	45



# NOLTR 72-15

## TABLES

Table	Title	Page
A1	Samples of the Three Component Model Prepared in the Patterson-Kelly Twin Shell Blender with ceramic Balls for Milling. Composition: 25 $\mu$ AP/Carnauba Wax/14 $\mu$ HMX, 71/20/9 .....	A-10
A2	Operations in the Preparation of Experimental Charges of AP N-139 and Aluminum (90/10) and Results .....	A-14
A3	Detonation Velocity Data from Fine APs at $d = 50.3$ mm .....	A-15
B1	Least Square Fits to HBX-1 Data <sup>6,7</sup> in Form $D(\text{mm}/\mu\text{sec}) = a(u) + b(u)$ .....	B-3
B2	Detonation Velocity Data for TNT/Al, 67.8/32.2 $\rho_v \approx 1.89$ g/cc .....	B-4
C1	Effect of Aluminum on Detonation Rate of Three Explosives ( $d = 5.08$ cm) .....	C-2

## EXPLOSIVE BEHAVIOR OF ALUMINIZED AMMONIUM PERCHLORATE

A systematic study of models of composite propellants was initiated several years ago. Detonability, shock sensitivity, and detonation velocity were investigated as a function of loading density ( $\rho_0$ ) and charge diameter ( $d$ ). Previous work included the study of ammonium perchlorate (AP)<sup>1,2</sup> and that of AP/wax mixtures<sup>3</sup>. The present work is a continuation of the original study and presents results for AP/Al mixtures in the range of 5-20% Al. Intended to be equally systematic, it is, however, less complete because funding from DOD for the work was terminated. It is the purpose of this report to organize and present the available results from work completed prior to the termination.

To study the simple composite model, AP/wax, we used AP of an average particle size of  $25\mu$ . In the course of the present work, we have learned to handle and mix fine APs with fine Al. Consequently most of the data reported here are for mixtures in which the particle size is  $10\mu$  or less and  $7\mu$ , respectively, for AP and Al. Despite the finer state of the components, replacement of the volatile fuel (wax) with aluminum produced complications.

We had found for pure AP that although the detonation velocity ( $D$ ) vs  $d^{-1}$  data were linear, their extrapolation to  $d^{-1} \rightarrow 0$  gave values of  $D$  too high to lie on the infinite diameter velocity  $D$  vs  $\rho_0$  curve derived for compactions at or below 52% TMD.<sup>2</sup> On the other hand, consistent and reasonable results were obtained at 55 and 67% TMD for waxed AP.<sup>3</sup> Successful extrapolation of data from the more greatly compacted charges of AP/wax was attributed to the higher reaction temperature and hence faster reaction; these are the results of the additional energy produced by the fuel/oxidant reaction. Because the literature contains qualitative statements indicating that Al and wax have similar effects on the detonability of AP, we first tried working at the same two compactions we had used for AP/wax. That procedure resulted in an apparent  $D_1$  vs % TMD curve for AP/Al, 95/5, intersecting the pure AP curve at 45% TMD, i.e., showing that Al increased  $D_1$

at a % TMD > 45% and decreased it otherwise. Check determinations of D at 40% TMD with 51 mm diameter charges contradicted this result; the velocity exhibited by AP/Al was definitely greater than that of AP. Consequently, a more complete study of D ( $\rho_o$ , d) had to be made for the aluminized APs than for the waxed APs. It showed that restriction of extrapolation procedures to % TMD  $\leq$  55% produced acceptable  $D_1$  values of AP/Al mixtures.

Aluminized AP exhibits Group 2 explosive behavior<sup>4</sup> as do waxed and pure AP. Al added to AP increases detonability (decreases critical diameter  $d_c$ ) and increases D to its maximum value at about 10% Al. The maximum increase is only about half that attained with wax as the fuel. The effect of Al on the D ( $\rho_o$ , d) pattern of AP is the opposite of its effect on organic high explosives.

## EXPERIMENTAL

### Materials

All AP used was propellant grade and contained 0.2% tricalcium phosphate. It was ground at the Naval Ordnance Station (Indian Head, Md.), and all fine APs were ground under the same schedule. The lots of AP used and their mean particle size by micromerograph are: N136(7.7 $\mu$ ), N138(8.4 $\mu$ ), N139(8.8 $\mu$ ), N141(7.2 $\mu$ ), N144(9.3 $\mu$ ), and N142 (22 $\mu$ ). All but the last, i.e., all the fine APs, are treated as equivalent. It has been shown<sup>5</sup> that N136 and N138 fall on the same D vs  $\rho_o$  curve for 51 mm dia. charges. It has subsequently been found\* that N139 and N141 fall on a second curve, parallel to the first, and 0.03 mm/ $\mu$ sec below it. An increase rather than a decrease would be expected because N141 has the smallest particle size. However, the change is experimentally insignificant. Finally, N141 and N144 are compared in AP/Al, 95/5 — :es (See Table 1). The D vs % TMD curves at d = 51 mm are parallel and separated by 0.06 mm/ $\mu$ sec. Again the difference is not significant.

---

\*Data in Appendix A

The aluminum used was dichromated spherical powder supplied in two batches (H-5 and H-30) by Valley Metallurgical Processing Company. The H-5 has an average particle size of  $7\mu$  by Fisher sub-sieve sizer, 99.12% through a No. 325 sieve, 94.6% free Al\*, 0.86% chromate, and 2.22%  $Al_2O_3$ . The H-30, analyzed in similar fashion, averages  $19.4\mu$ , 99.8% through No. 200 sieve 83.6% through a No. 325 sieve, 99.0% free Al, 0.09% chromate, and 0.88%  $Al_2O_3$ . Similar batches which had been stored at NOL for a year showed higher  $Al_2O_3$  content.

Al has a melting point of  $634^\circ C$  and a boiling point of  $2422^\circ C$  in contrast to the relatively volatile fuel, carnauba wax, which has a boiling point of  $320^\circ C$ .

#### Charge Preparation and Experimental Procedure

Mixtures of fine AP and fine Al were prepared in batches of one kilogram. The mixing was carried out in a paint can shaker which also contained 0.5 kg of 12 mm dia ceramic balls. Although the AP is, of course, stored under desiccant, the weighing and mixing can be carried out under ambient conditions. The loose powder should appear uniform after mixing; if it does not, it must be discarded, for only gross agglomeration of the AP causes detectable non-uniformity at this stage. Our usual test of adequate dispersal is preparation, by isostatic pressing, of a compacted plug which is then machined into a cylindrical charge. Only if the machined surface seems uniformly gray can the original mixture be considered completely satisfactory. If aggregates of AP appear as white specks on the surface, their size and number determine whether the charge is fired or rejected. For example, a 3.5 cm dia x 22.9 cm long charge showing 6 specks of an average size of  $125\mu$  (largest  $200\mu$ ) is considered a good one.

A good mixing operation is of basic importance to the quantitative study; Appendix A goes into detail about the development of the one we have used here. At first (and for the 90/10 AP/Al data reported), a sufficient number of the small (1 kg) batches were blended in a

-----  
\*Manufacturer's analysis; manufacturer's specifications are for 97.5% or more free Al.

rotating barrel to provide a large batch sufficient for the entire investigation. However, charges from the large batch showed more specks than those from small ones. The blending operation was therefore discarded and subsequent work was carried out on freshly prepared small batches.

All charges were either unconfined or supported in 0.08 mm-thick cellulose acetate. They were compacted by hand (h), by hydraulic press (H), or by isostatic press (i). The method used is indicated by the letter following the density in the tables. All charges were conditioned at 25°C before firing. Good streak camera records were obtained when we used the hand packed or isostatically pressed (and subsequently machined) charges. When we used those of intermediate density which had to be prepared with the hydraulic press, the records were occasionally poor. In this case, the mixture is compacted into pellets of length equal to the diameter. The charge then consists of the necessary number of pellets to make up the charge length of 22.8 cm. Each pellet was somewhat non-uniform because of the method of compaction; it was sometimes difficult to align the pellets properly; and even proper alignment could not eliminate the interfaces between pellets. Some records from such charges were less satisfactory than others, and a number had to be discarded, e.g., when the trace from each pellet of the charge showed a different slope. All charges were conditioned at 25°C before firing.

Charges were of various diameters up to 7.62 cm and were 22.8 cm long. Boosters were of 50/50 pentolite (1.56 g/cc), of the same diameter as the charge, and 2.54 cm long. A pentolite witness was frequently placed at the end of the charge. The shock-induced disturbance was recorded by a 70 mm streak camera at writing speeds of 1 to 4 mm/ $\mu$ sec. Streak camera records were similar to those of previous work<sup>1</sup>; a typical record is shown in Fig. 1.

Record reduction was carried out as in previous work<sup>1,3</sup>. The average precision of the replicates in the 95/5 series was 0.3% with a range of 0.1 - 0.7%; in the 90/10 series, 0.7% with a range of 0.1 - 1.5%. These results reflect the better charge preparation achieved

1.0 LTR. P-15



FIG. 1 TYPICAL STELLAR RECORD, SHOT 023 OF AP AL, 25.5, AT  $\rho_0 = 1.037 \text{ g cc.}$

in the former series as well as an improvement over the waxed AP mixtures.<sup>3</sup>

## RESULTS AND DISCUSSION

### Detonation Velocity Relationships

AP/Al, 95/5. Table 1 contains the data obtained on the fine AP/Al, 95/5, mixtures. They are plotted  $D$  vs % TMD in Fig. 2. [The ratio of charge density to its voidless density is defined as  $\Delta$ . The percent theoretical density (% TMD) is  $100 \Delta$ .] The curves of Fig. 2 show a typical explosive Group 2 behavior, fanning out from some point at low  $\Delta$  and exhibiting a maximum in  $D$  prior to reaching the failure or critical  $\Delta$ . They also demonstrate very clearly why extrapolations of  $D$  vs  $d^{-1}$  at 67% TMD gave unacceptable results for  $D_1$ ; the  $D$  vs % TMD curves are linear only in the range 40 - 55% TMD and  $d > 2.54$  cm.

Extrapolations of  $D$  vs  $u$  (the notation  $u = d^{-1}$  is introduced here for convenience) data were carried out at 40.5% and 55.0% TMD. They are shown in Fig. 3 where the plotted data points are from Table 1 and straight lines are a least squares fit to the data which gives

$$D = 3.454 - 13.40 u, \Delta = 0.405 \quad (1)$$

$$D = 4.286 - 17.85 u, \Delta = 0.550 \quad (2)$$

All 40.5% TMD data were included to derive Eq. (1) since Fig. 2 shows all  $D$  vs  $\Delta$  curves linear at the lower  $\Delta$  value. At 55.0% TMD, however, the values at  $d = 19.1$  mm ( $u = 0.0524 \text{ mm}^{-1}$ ) lie on the curved portion of the  $D$  vs  $\Delta$  curve of Fig. 2 and hence were omitted from the fit of the  $D$  vs  $u$  data; as would be expected, they fall below the curve in Fig. 3b.

Neither Fig. 3a nor 3b shows any sign of a sharp change in slope such as that found in the  $D$  vs  $u$  curves of mixtures of AP with the volatile fuels, wax and HMX.<sup>3</sup> With the assumption that the infinite diameter detonation velocity ( $D_1$ ) is a linear function of  $\Delta$ , the extrapolations of Fig. 3 give

NOLTR 72-15

TABLE 1

DETONATION VELOCITY MEASUREMENTS ON AP/A1, 95/5

( $\rho_v = 1.98$  g/cc)

Shot No.	d cm	$\rho_o$ g/cc	$\Delta$	D mm/ $\mu$ sec	Comment
AP-141 (7.2 $\mu$ )					
882	5.08 ↓ ✓	0.801H	0.405	3.268	
883		1.001H	0.506	3.756	
884		1.1451	0.579	4.133	
879		1.2681	0.641	4.405	
880		1.3251	0.670	4.517	
881		1.4611	0.739	4.506	
885		1.5331	0.775	(4.148)	Failing, Near critical
885A		1.5951	0.807	F	
AP-144 (9.3 $\mu$ )					
924	0.635	0.801h	0.405	F	
923	0.952	0.804h	0.407	2.065	
914	1.27	0.808H	0.409	2.34-9	Poor trace
925	↓	0.994H	0.503	Go*	No record**
915		1.087H	0.550	F	No trace
918		1.088H	0.550	F	No trace
910	1.91	0.804H	0.407	2.761	
911	↓	1.088H	0.550	3.231	
916		1.088H	0.550	3.212	
921		1.211H	0.613	3.118	
919		1.267H	0.641	F	
920	↓	1.325H	0.670	F	
913		1.260H	0.637	3.356	
922		1.324H	0.670	F	
912	2.40	1.267H	0.641	3.479	
912A	↓	1.325H	0.670	F	No trace
917		1.325H	0.670	3.275	
905	2.54	0.80H	0.405	2.914	
908	↓	0.80H	0.405	2.922	
892		1.087H	0.550	3.562	
893		1.087H	0.550	3.612	
899		1.267H	0.641	3.682	
898		1.326H	0.671	3.287	



TABLE 1 (Cont.)

DETONATION VELOCITY MEASUREMENTS ON AP/A1, 95/5  
( $\rho_v = 1.98 \text{ g/cc}$ )

Shot No.	d cm	$\rho_o$ g/cc	$\Delta$	D mm/ $\mu$ sec	Comment
AP-144 (9.3 $\mu$ )					
906	3.47	0.80H	0.405	3.060	
894	↓	1.087H	0.550	3.757	
901		1.267H	0.641	4.053	
900		1.326H	0.671	4.066	
926	↓	1.471H	0.744	F	No record**
907	5.08	0.80H	0.405	3.194	
887	↓	0.801H	0.405	3.199	
888		1.001H	0.506	3.729	
895		1.087H	0.550	3.955	
886		1.205H	0.610	4.208	
897		1.267H	0.641	4.356	
889		1.2671	0.641	4.376	
902		1.325H	0.670	4.413	
932		1.325H	0.670	4.442	
890		1.3901	0.703	4.485	
891		1.5041	0.761	4.338	
927		1.541H	0.779	Go*	
909	7.62	0.80H	0.405	3.280	
896	↓	1.087H	0.550	4.038	
904		1.267H	0.641	4.529	
903		1.325H	0.670	4.674	
928		1.400H	0.708	4.769	
929		1.500H	0.759	4.916	
930		1.600H	0.809	(4.4)	Failing-near critical
931	↓	1.700H	0.860	F	

\*Set off explosive witness of pentolite 50/50

\*\*Electronic instrument failure.

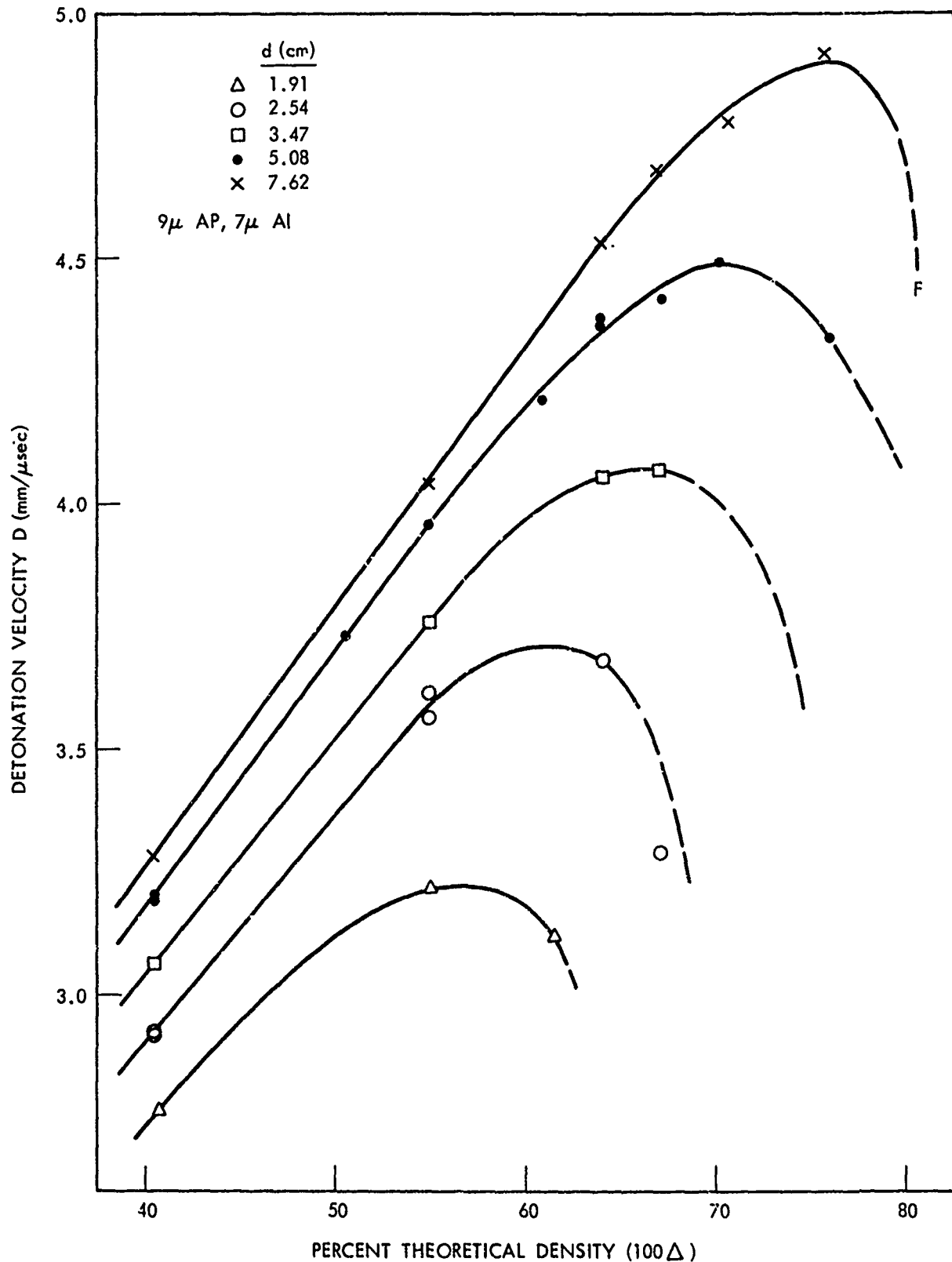


FIG. 2 EFFECT OF CHARGE DENSITY AND DIAMETER ON DETONATION VELOCITY OF AP/Al, 95/5

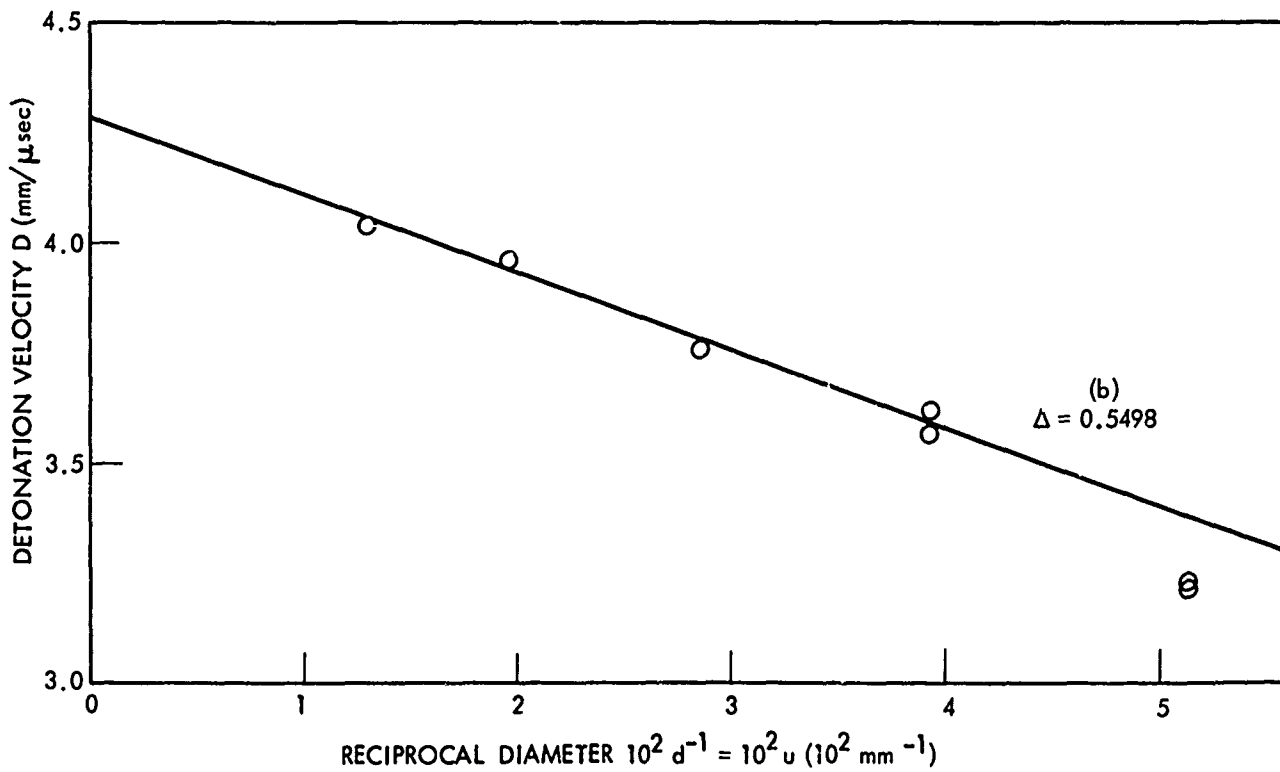
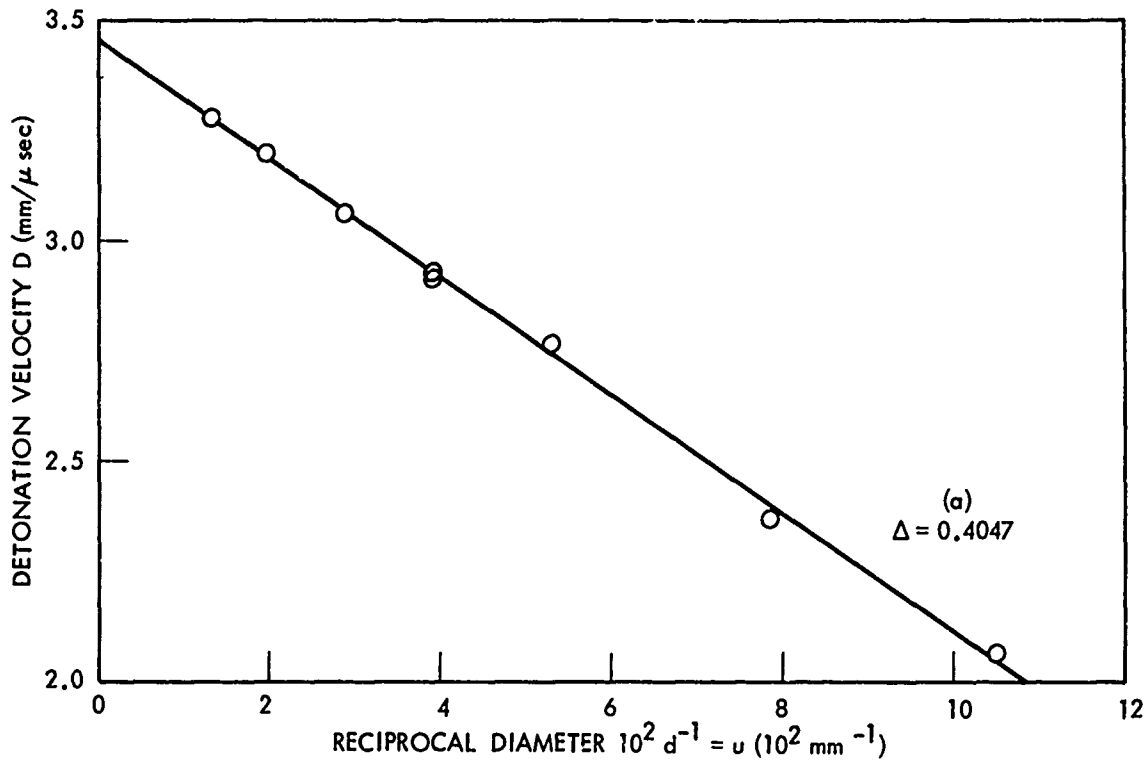


FIG. 3 EXTRAPOLATION TO INFINITE DIAMETER DETONATION VELOCITY OF AP/Al, 95/5, DATA

$$D_1 = 1.134 + 5.734 \Delta \quad (3)$$

for 95/5, AP/A1.

In reference 4 it was remarked that the D vs  $\Delta$  curves for the Group 1 explosives (TNT and HBX-1) fanned out from a common D value at  $\Delta \sim 1.0$  with slopes increasing linearly with  $u^*$ , and that analogous Group 2 curves seemed to have a common point at some low  $\Delta$  and to fan out from it with slopes which decreased with  $u$ . Our work with AP<sup>1,2</sup> and with AP/wax<sup>3</sup> did not extend over a sufficient range of small  $\Delta$  values to demonstrate the linear portion of the D vs  $\Delta$  curve. Hence AP/A1, 95/5, provides the first example for which this trend can be shown quantitatively. Table 2 presents equations for the linear portions of the D vs  $\Delta$  curves of Fig. 2 in the form

$$D = a(u) + b(u)\Delta \quad (4)$$

Fig. 4 shows that the plots of the coefficients  $a(u)$  and  $b(u)$  are linear functions of  $u$ . The points shown are values from Table 2 (obtained from graphically smoothed curves of Fig. 2); the lines are from the analytically smoothed data of Fig. 3. The final result of the smoothing is then

$$a(u) = 1.134 - 0.99 u = a_0 - 0.99 u \quad (5)$$

$$b(u) = 5.734 - 30.67 u = b_0 - 30.67 u \quad (6)$$

so that the general expression for D of this particular mixture is

$$D(\Delta, u) = 1.134 - 0.99 u + (5.734 - 30.67 u)\Delta \quad (7)$$

with a common point at  $\Delta \sim -0.03$ . At infinite diameter,  $u = 0$ , and Eq. (7) reduces to Eq. (3) applicable to any 95/5, AP/A1 mix.

General Relations for  $D(\Delta, u)$ . The treatment of the AP/A1, 95/5, data above was a specific example of some useful general relationships which will now be given for subsequent use. Wherever we can show

---

\*A common point in the D- $\Delta$  plane and linear variation of the slope with  $u$  implies linear variation of the intercept with  $u$ .

TABLE 2

COEFFICIENTS FOR LINEAR PORTION OF D vs  $\Delta$  CURVES OF AP/A1, 95/5

<u>d (mm)</u>	<u>u (mm<sup>-1</sup>)</u>	<u>D (mm/μsec)</u>	
		<u>a (u)</u>	<u>b (u)</u>
25.4	0.03937	1.06	4.59
34.7	0.02882	1.12	4.78
50.8	0.01969	1.11	5.16
76.2	0.01312	1.14	5.293
∞	0.0	1.134	5.734

AP 144 (9.3μ)

A1 H5 (7μ)

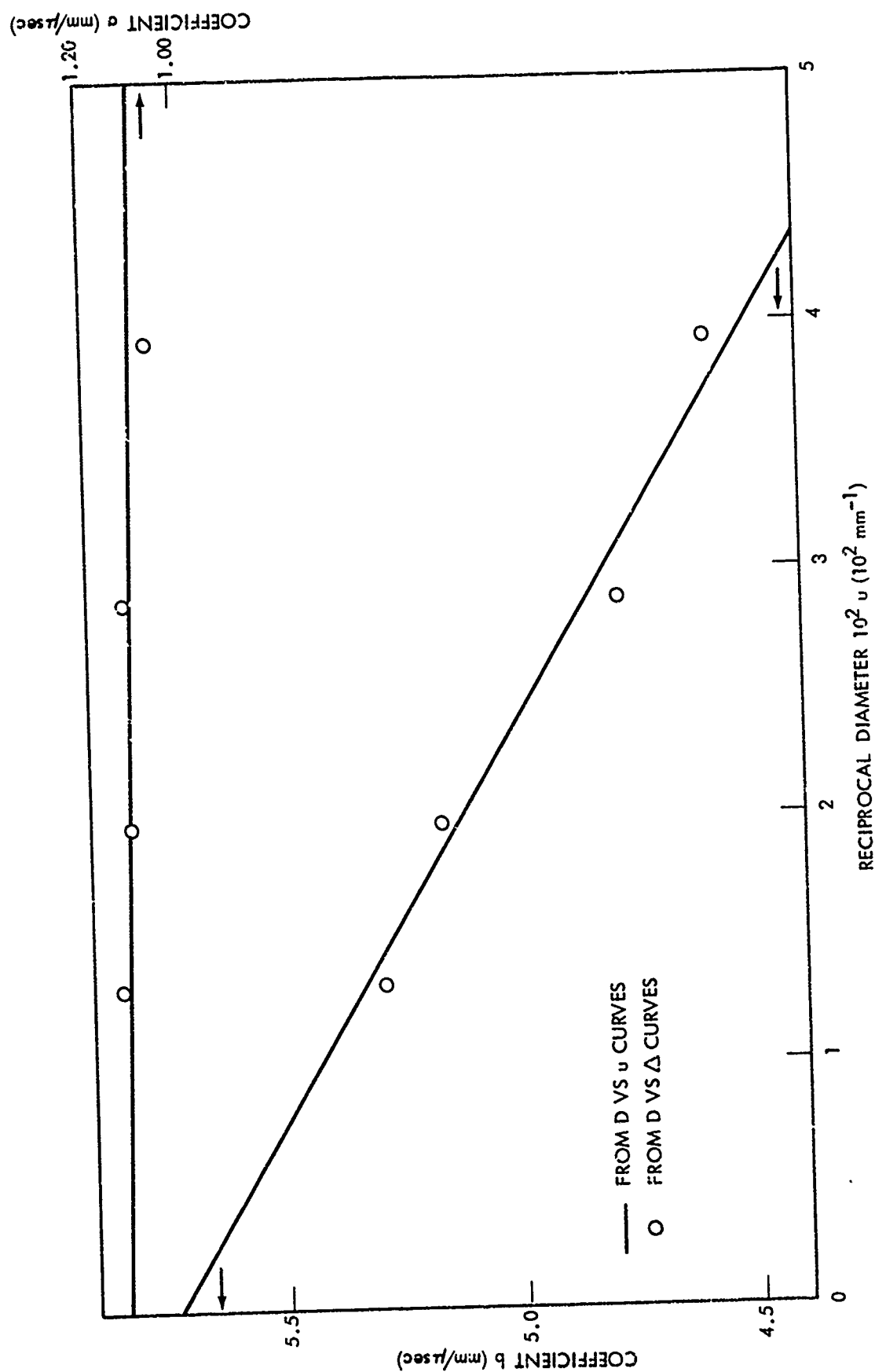


FIG. 4 VARIATION OF COEFFICIENTS OF  $D$  VS  $\Delta$  CURVES FOR AP/Al, 95/5, WITH RECIPROCAL DIAMETER

empirically that  $D$  is a linear function of  $\Delta$  at a given  $u$  (and hence  $u$ ), we assume that the coefficients are functions of  $u$  only so that

$$D(\Delta, u) = a(u) + b(u)\Delta. \quad (8)$$

Moreover, when  $D$  is a linear function of  $u$  for a given  $\Delta$ , the analogous relation is

$$D(\Delta, u) = a_0 + b_0 \Delta + \beta(\Delta) u \quad (9)$$

where the subscript zero refers to the infinite diameter ( $u = 0$ ) values of the coefficients in Eq. (8). Differentiation of Eq. (8) gives

$$\left(\frac{\partial D}{\partial u}\right)_\Delta = a' + b' \Delta \quad (10)$$

where the prime indicates a derivative with respect to  $u$ . By definition,  $\beta(\Delta) = (\partial D / \partial u)_\Delta$ ; hence Eq. (10) can be written

$$\beta(\Delta) = a' + b' \Delta \quad (11)$$

Since for any given  $\Delta_1$ , we find  $D(\Delta_1, u)$  vs  $u$  linear,  $\beta(\Delta_1)$  must be a constant. Hence  $a'$  and  $b'$  must be constants; in other words,  $a(u)$  and  $b(u)$  are linear functions of  $u$ , and, as Eq. (11) shows,  $\beta(\Delta)$  is a linear function of  $\Delta$ . Moreover, equating the right hand side of Eq. (8) at two specific values of  $u$  shows intersection of the  $D$  vs  $\Delta$  curves at a value of

$$\Delta_0 = -a'/b'. \quad (12)$$

If the required linear relationships are known (or assumed) to exist, Eq. (11) is particularly useful. Two  $D$  vs  $u$  curves [Eq. 9] define  $a_0$ ,  $b_0$ , and two values of  $\beta(\Delta)$ ; the last in Eq. (11) define  $a'$  and  $b'$  and hence the general equation

$$D(\Delta, u) = a_0 + a'u + (b_0 + b'u)\Delta \quad (13)$$

applicable to the specific explosive used. The same process can be followed with two  $D$  vs  $\Delta$  curves, but, as with AP/A1, 95/5, smoothing the  $D$ - $u$  curves seems to produce better results. This stems, in part, from the greater amount of data available from detonability

determinations and, in part, from the more reliable linearity of the D-u curves; they are frequently linear when the D-Δ curves are not. It should be noted, however, that the above relations apply only when there is linearity in both planes, the D-Δ as well as the D-u. The coefficients  $a_0$  and  $b_0$  are chemical characteristics of the explosive, but the parameters  $a'$  and  $b'$  depend very strongly on physical properties such as initial particle size distribution and shape.

AP/Al, 90/10. It has already been mentioned that because of differences in preparing the mixtures, results for AP/Al, 90/10, are more scattered and somewhat less precise than those for the 95/5 mixture. They are quite adequate, however, to demonstrate the same behavior pattern for both mixtures.

Table 3 contains the data for AP/Al, 90/10. and Fig. 5 shows plots of D vs Δ for various diameters. As in the case of the 95/5 mixture, it is a typical Group 2 behavior with D-Δ curves fanning out from some small Δ value and a slope which increases with increasing d. The curves of Fig. 5 were graphically smoothed and values from the smoothed curves at Δ values of 0.309, 0.354, 0.399, 0.450, and 0.499 were used to construct D-u curves; three are shown in Fig. 6. The intercepts ( $u = 0$ ) of these curves were then used to obtain

$$D_1 = 1.130 + 6.107 \Delta \quad (14)$$

for 90/10, AP/Al.

Table 4 contains the coefficients for the linear portions of the D-Δ curves (Fig. 5) and Fig. 7 shows the variation of these coefficients with u. Equations for the straight lines of Fig. 7 are given at the bottom of Table 4. These lead to the general expression for D of the 90/10 mix:

$$D(\Delta, u) = 1.13 + 7.76 u + (6.107 - 43.7 u) \Delta . \quad (15)$$

The 90/10, AP/Al, mix was also used in a brief investigation of the effect of particle size on D. The data are collected in Table 5, and plotted for two diameters in Fig. 8. Comparisons were made in the range 40-55% TMD where D-Δ curves are linear for the control mix with



NOLTR 72-15

TABLE 3

DETONATION VELOCITY MEASUREMENTS ON AP/A1, 90/10  
( $\rho_v = 2.006$ , AP-141, 7.2 $\mu$ )

Shot No.	d cm	$\rho_o$ g/cc	$\Delta$	D mm/ $\mu$ sec	Comment
844	2.54 ↓	0.621h	0.310	2.710	
845		0.621h	0.310	2.746	
846		0.901h	0.449	3.313	
847		0.901h	0.449	3.318	
810		1.103H	0.550	3.782	
811		1.103H	0.550	3.773	
826		1.107H	0.552	3.792	
853		1.2691	.633	4.088	
828		1.3451	.670	---	No trace
805		1.3491	.672	4.080	
806		1.3501	.673	4.070	
827		1.3611	.678	4.102	
852		1.4091	.702	3.844	
864		1.4311	.713	F	No trace, H.E. recovered
862		1.4761	.736	F	
847		1.4811	.738	F	
832	3.49	0.619h	0.309	2.816	
849	3.49	0.859h	0.428	3.269	
859	3.49	0.904h	0.450	3.626	Trace in 2 sections and wavy**
812	3.48	1.103H	0.550	3.914	
829	3.48	1.105H	0.551	3.963?	Charge pellets (6) not parallel
807	3.49	1.3491	0.672	4.451	
863	4.99	0.901h	0.449	3.649	3.654*
860	4.99	0.904h	0.451	3.539	3.544*
833	5.08 ↓	0.620h	0.309	2.886	
850		0.783h	0.390	3.283	
813		1.103H	0.550	4.122	
830		1.103H	0.550	4.052	
808		1.3461	0.671	4.689	
809	7.32	1.3561	0.676	4.883	4.887*
861	7.49	0.904h	0.451	3.769	3.771*
834	7.62 ↓	0.620h	0.309	2.947	
851		0.688h	0.343	3.058	
820		1.096H	0.546	4.039	Trace in two sections**
				4.098	
814	↓	1.104H	0.550	4.242	
831q		1.104H	0.550	4.138	

\*Corrected to group diam. of 5.08 or 7.62.

\*\*Point discarded.

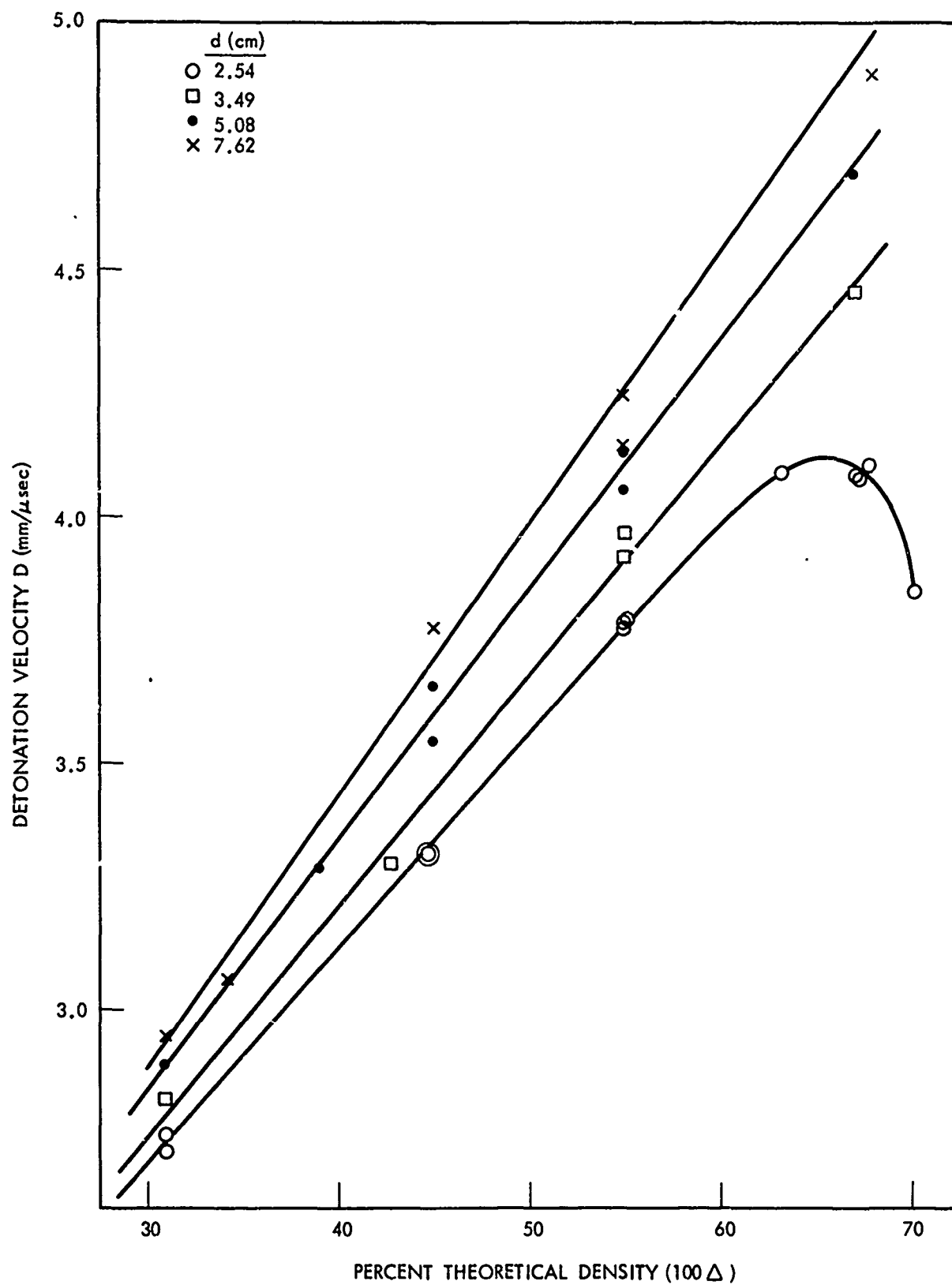


FIG. 5 EFFECT OF CHARGE DENSITY AND DIAMETER ON DETONATION VELOCITY OF AP/Al, 90/10

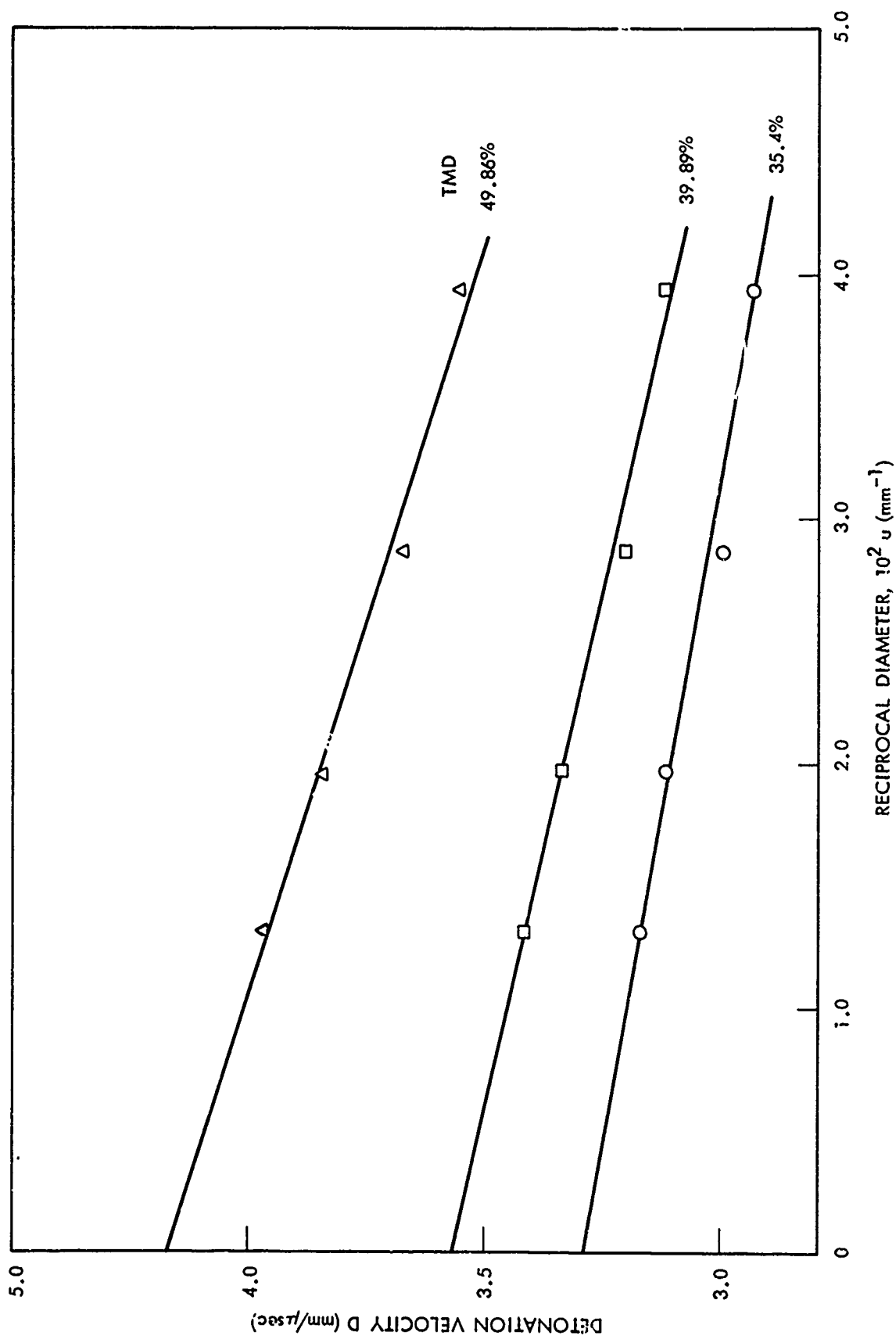


FIG. 6 EXTRAPOLATION OF SMOOTHED DATA OF AP/AI, 90/10, TO INFINITE DIAMETER DETONATION VELOCITY

TABLE 4

COEFFICIENTS FOR LINEAR PORTION OF D vs  $\Delta$  CURVES FOR AP/A1, 90/10

<u>d (mm)</u>	<u>u (mm<sup>-1</sup>)</u>	<u>D (mm/<math>\mu</math>sec)</u>	
		<u>a (u)</u>	<u>b (u)</u>
25.40	0.03937	1.38	4.357
34.95	0.02863	1.35	4.648
50.80	0.01969	1.33	5.041
76.20	0.01312	1.23	5.504
$\infty$	0.0	1.13	6.107

$$a(u) = 1.130 + 7.76 u$$

$$b(u) = 6.107 - 47.3 u$$

AP N141 (7.2 $\mu$ )

A1 H5 (7 $\mu$ )

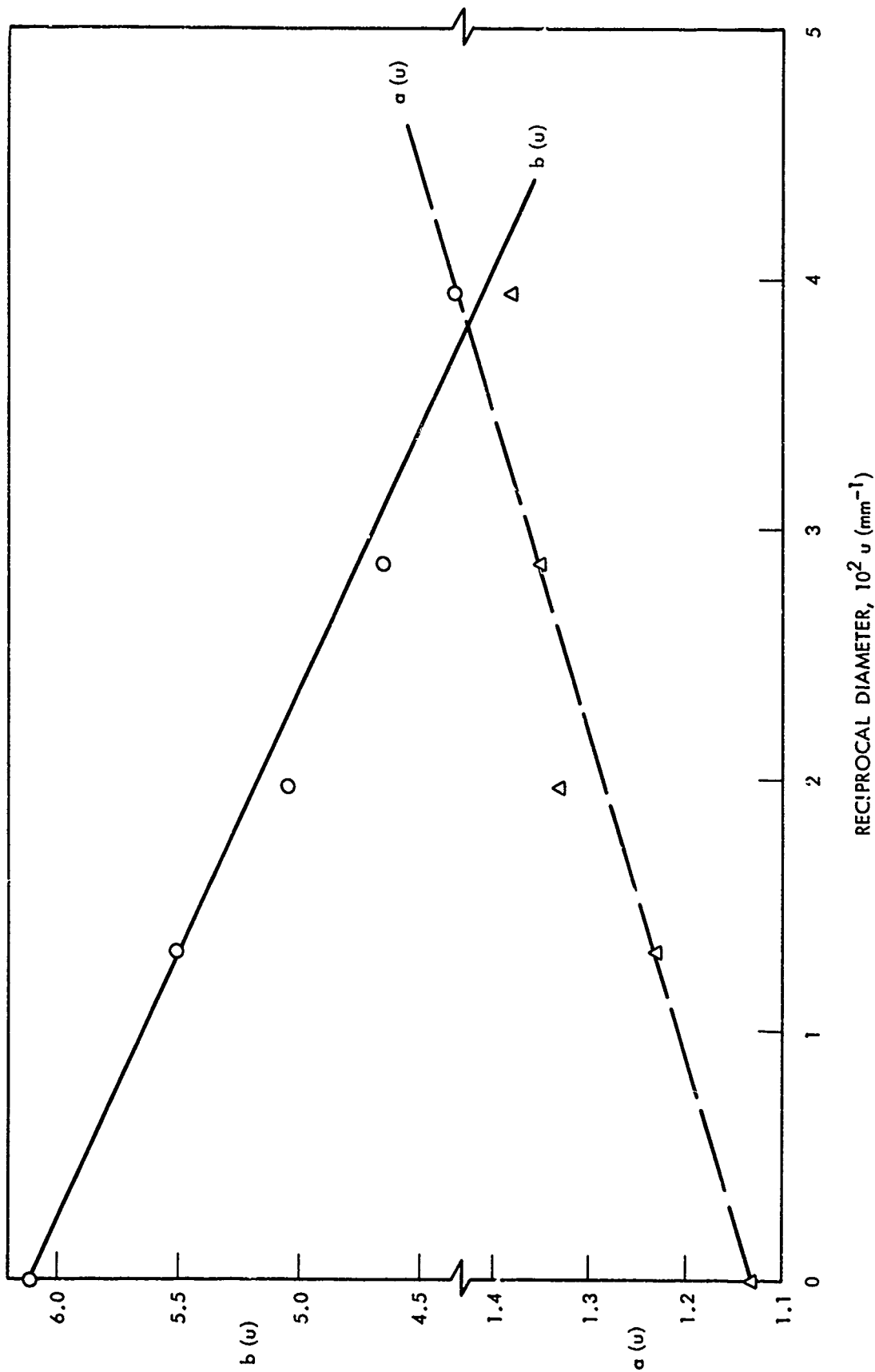


FIG. 7 VARIATION OF COEFFICIENTS OF D VS  $\Delta$  CURVES FOR AP/AI, 90/10, WITH RECIPROCAL DIAMETER

smallest particle size components. Solid lines show Eq. (15) at the indicated  $d$  and  $\Delta$  for  $7\mu$  AP and  $7\mu$  Al; dashed lines are estimates from the few data of Table 5 for  $22\mu$  AP and  $7\mu$  Al; solid points are for  $8\mu$  AP and  $19\mu$  Al. As Fig. 8 illustrates, increasing the particle size of either component decreases the detonation velocity exhibited by the mixture. About the same increase (to ca. 3x original dia) has approximately twice the effect when made for the oxidizer AP rather than when made for the fuel, Al.

It is of interest that the D-u curves from the few data of Table 5 for mixtures with  $22\mu$  AP and  $7\mu$  Al do not extrapolate to  $D_1$  values given by Eq. (15) unless a marked change in the slope of the D-u curve is assumed. As remarked earlier, such a change has been observed for AP/wax and AP/HMX, but did not appear in data for the fine mixes of AP/Al. D values for 76 mm dia charges tended to be erratic here as they did also for the fine mixes. This is attributed in all cases to the difficulty of preparing good charges of this size with our equipment as well as to assuming the equivalence of the observed peripheral front with that on axis. (The latter assumption was made for charges of all sizes, but the discrepancy between progress of the front on axis and at the charge boundary increases with increasing charge diameter.)

AP/Al, 80/20. The initial work on the 80/20 mix was with charges compacted to 55% TMD in the hydraulic press. Satisfactory records were obtained from them. However, records from charges hydraulically pressed to 40% TMD were virtually worthless and were consequently discarded. At the lower density, we found that charges hand packed in cellulose acetate tubes produced sufficiently sharp records for measurements. These are therefore the ones reported in Table 6.

Very few shots were made with the 80/20 mix because the program was interrupted. From the two points obtained by extrapolating the D-u curves,

$$D_1 = 1.10 + 5.57 \Delta \quad (16)$$

for this 80/20 mix. If we assume that this mix shows the same set of

## NOLTR 72-15

TABLE 5

## EFFECT OF PARTICLE SIZE ON DETONATION VELOCITY OF AP/Al MIXTURES

Shot No.	d cm	$\rho$ g/cc	% TMD	D mm/ $\mu$ sec
AP(136)/Al-H30, 95/5				
621	2.54	1.088H	55.0	3.230
622	3.49	↓	↓	3.514
623	5.08	↓	↓	3.794
624	7.62	↓	↓	3.915
AP(142)/Al-H5, 90/10				
791	2.54	1.103H	55.0	3.278
792	↓	↓	↓	3.252
821	↓	↓	↓	3.217
822	↓	↓	↓	3.172
793	3.49	↓	↓	3.415
823	3.49	↓	↓	3.402
794	5.08	1.101H	54.9	3.643
824	5.08	1.103H	55.0	3.601
795	7.62	1.104H	↓	3.614
825	7.62	1.104H	↓	3.770
AP(136)/Al-H30, 90/10				
629	2.54	1.104H	55.0	3.458
630	3.49	1.104H	55.0	3.619
631	5.08	1.125H	56.1	3.957
632	7.62	1.104H	55.0	4.011
AP(142)/Al-H5, 90/10				
837	3.49	0.803h	40.0	2.851
838	3.49	↓	↓	2.869
839	5.08	↓	↓	2.864
843	7.62	0.814h	40.6	3.122

AP(136):8.4 $\mu$  by micromerographAP(142):22 $\mu$  by micromerographAl:H5 and H30 are respectively, 7 and 19.4 $\mu$  by Fisher sub-sieve sizer.

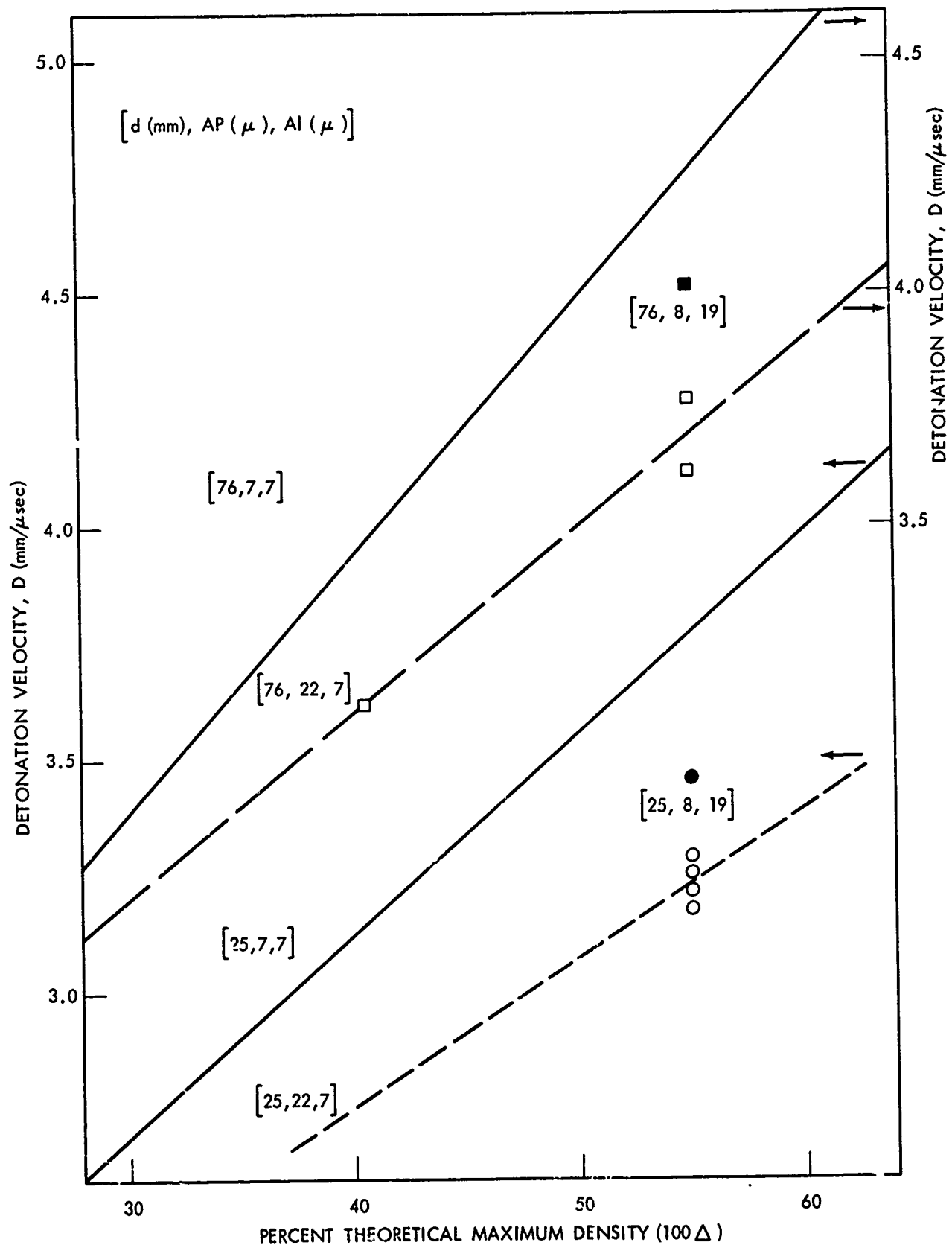


FIG. 8 EFFECT OF PARTICLE SIZE OF AP AND OF AI ON DETONATION VELOCITY OF AP/AI, 90/10



TABLE 6

DETONATION VELOCITY MEASUREMENTS ON AP/A1, 80/20  
( $\rho_v = 2.065 \text{ g/cc}$ )

Shot No.	d cm	$\rho$ g/cc	$\Delta$	D mm/ $\mu$ sec
947	3.49	0.826h	0.400	2.97*
948	5.08	0.826h	0.400	3.074
949	7.62	0.826h	0.400	3.175
936	2.54	1.136H	0.550	3.672
937	2.54	↓	↓	3.652
939	3.49			3.792
942	5.08			3.888
943	7.62			3.997

\*Record sharp but in two sections; slope of final section used.

AP 144:9.3 $\mu$

A1 H5:7 $\mu$

linear relations found for the 5 and 10% Al mixtures, its general equation would be

$$D(\Delta, u) = 1.10 - 10.3 u + (5.57 - 4.6 u)\Delta \quad (17)$$

Comparison of  $D(\Delta, u)$  for AP/Al with that of other composite explosives

The 90/10, AP/Al, mixture showed the largest effect of Al on detonation velocity; this mix will be used to illustrate the  $D(\Delta, u)$  behavior of aluminized AP. Eq. (15) describes the diameter and compaction effects on  $D$  as illustrated in Fig. 9. In this case the  $D-\Delta$  curves radiate from a common point of  $\Delta_0 \sim 0.16$  with slopes decreasing linearly as  $u$  increases (or as  $d$  decreases). The solid lines indicate the experimental range in  $\Delta$  and that area covered on a larger scale in Fig. 5. This is a quantitative example of the pattern described qualitatively in Reference 4.

There are very few diameter effect studies on aluminized organic H. E. The two of which the authors know are HBX-1<sup>4,6,7</sup> and Tritonal 67.8/32.2.<sup>7</sup> Both of these studies were carried out at NOL; some of the relevant data are given in Appendix B and the Group 1 pattern shown by the Tritonal appears in Fig. 10. In contrast to AP/Al, the curves coincide at high  $\Delta_0$  (ca. 1.12 in this case) and have slopes increasing with increasing  $u$ . The diameter effect is appreciably smaller than that found in aluminized AP, as might be expected.

In the study of waxed AP<sup>3</sup>, measurements were made at only two  $\Delta$  values (0.55 and 0.67) and it was assumed that the  $D-\Delta$  curves were linear in that region. The  $D-u$  curves generally showed a marked change in slope; only the upper segment (low  $u$  range) was used for extrapolation. If we choose AP/wax, 80/20, as representative of the waxed AP and assume linearity as before, the general relation is

$$D(\Delta, u) = 2.14 + 63.4 u + (4.95 - 173 u)\Delta, \quad u \leq 0.025 \quad (18)$$

Eq. (18) should generate a Group 2 pattern because the detonability behavior of waxed AP is of this group. It does, as Fig. 11 illustrates.

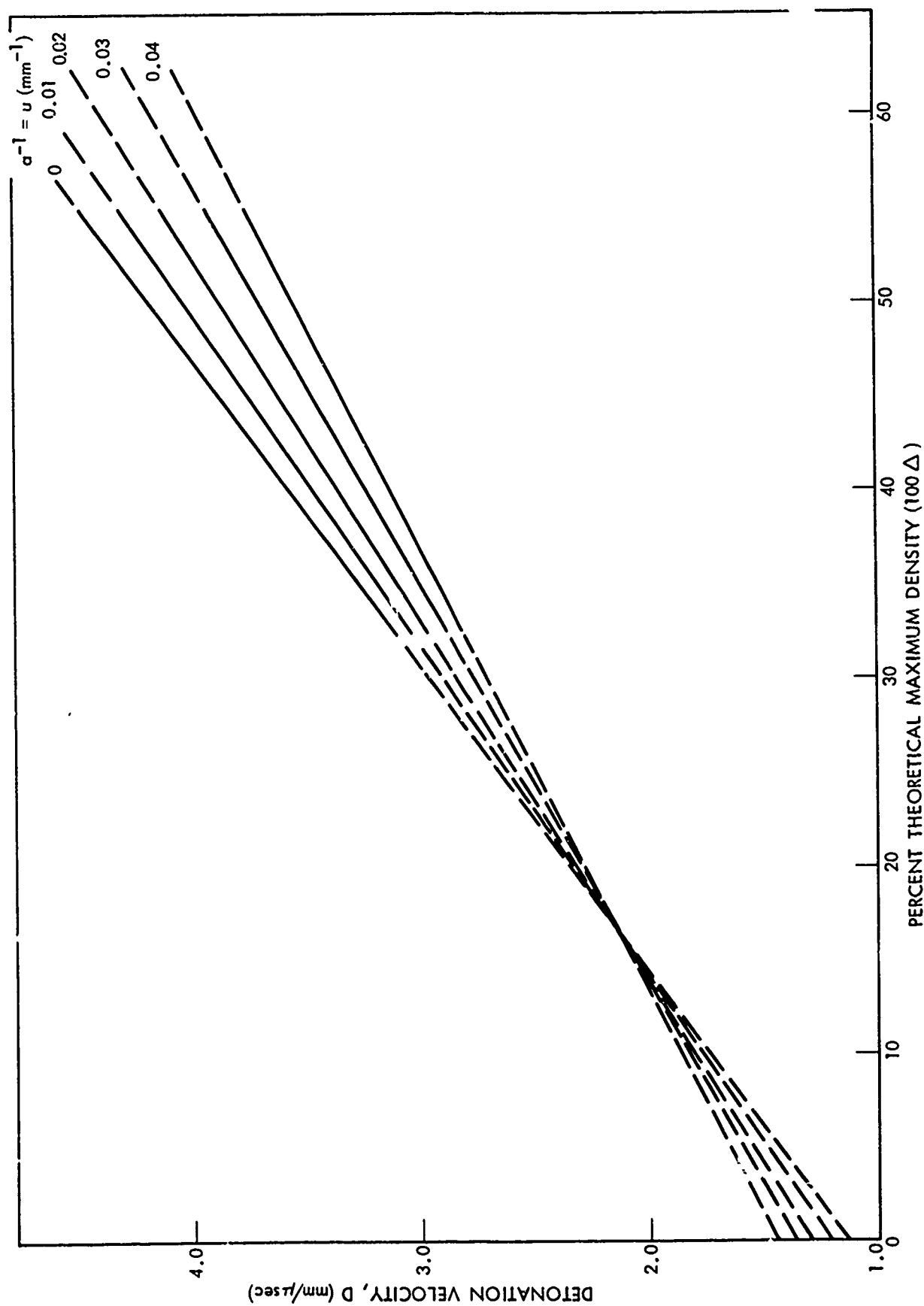


FIG. 9 EXPLOSIVE GROUP 2 BEHAVIOR OF AP/Al, 90/10

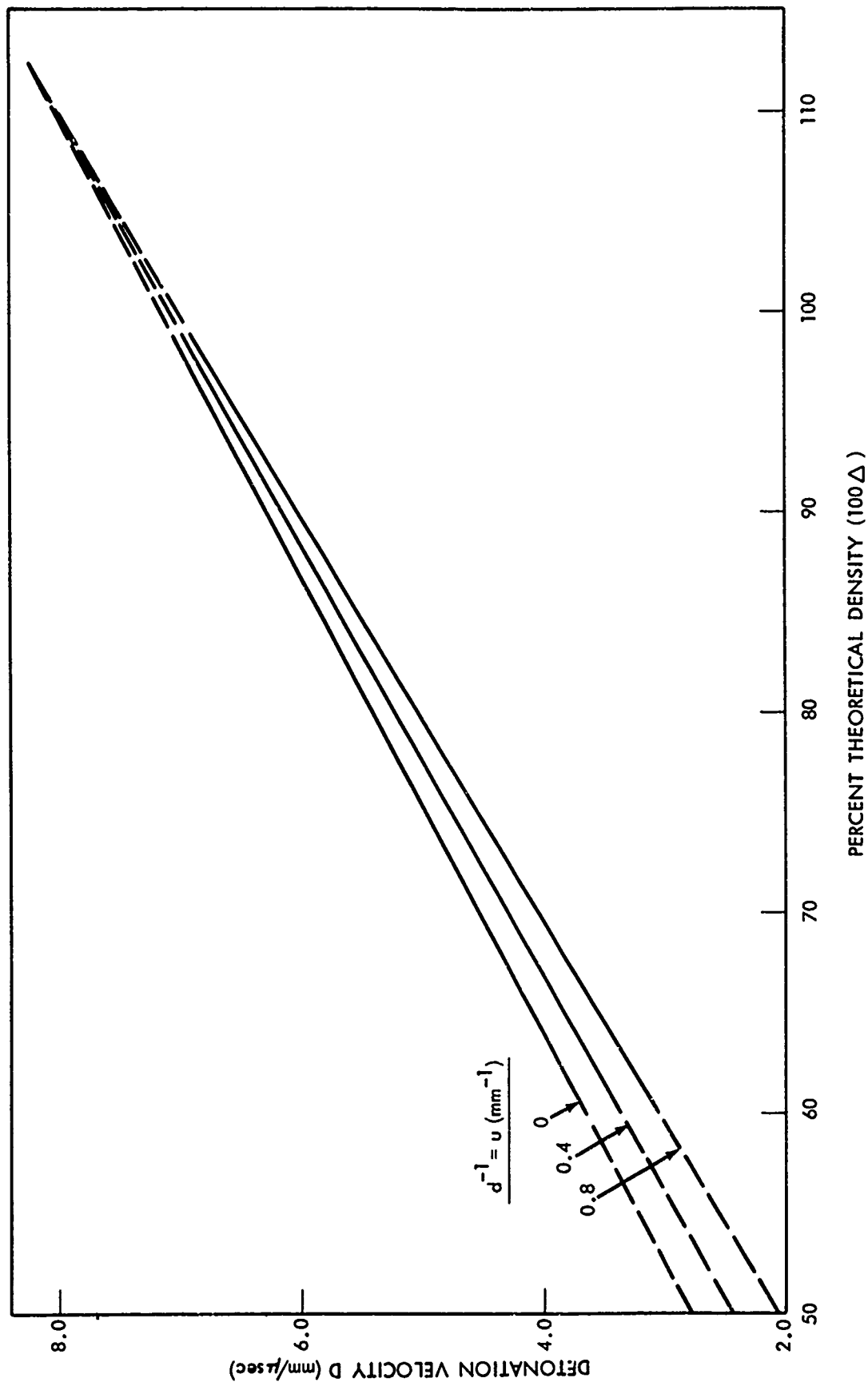


FIG. 10 EXPLOSIVE GROUP 1 BEHAVIOR OF TNT/Al, 67.8/32.2

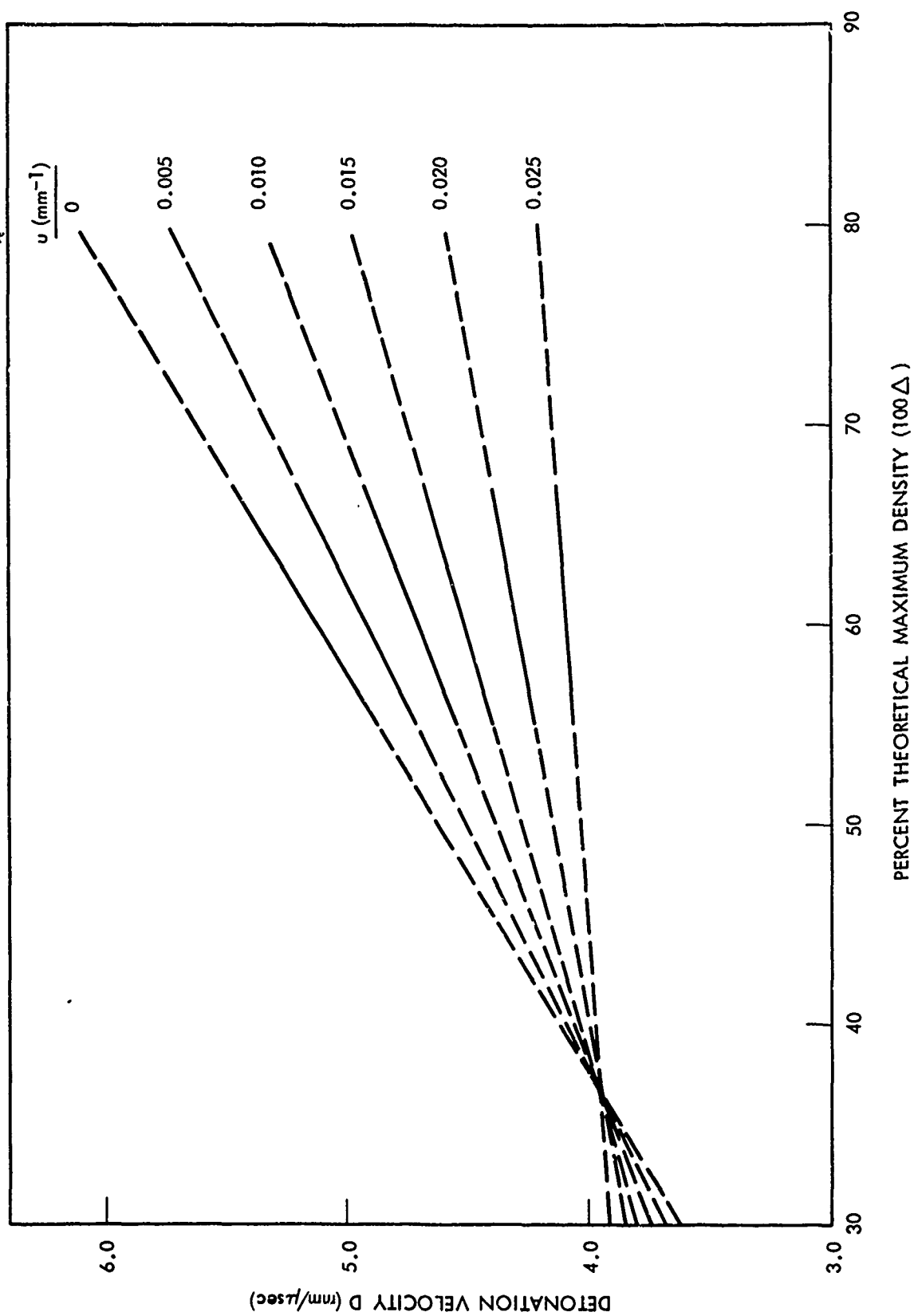


FIG. 11 EXPLOSIVE GROUP 2 BEHAVIOR OF AP/WAX , 80/20

The present data show that the mixture of the non-explosive fuels (wax or Al) with an explosive exhibits the group behavior of the explosive component, as originally proposed in Reference 4.

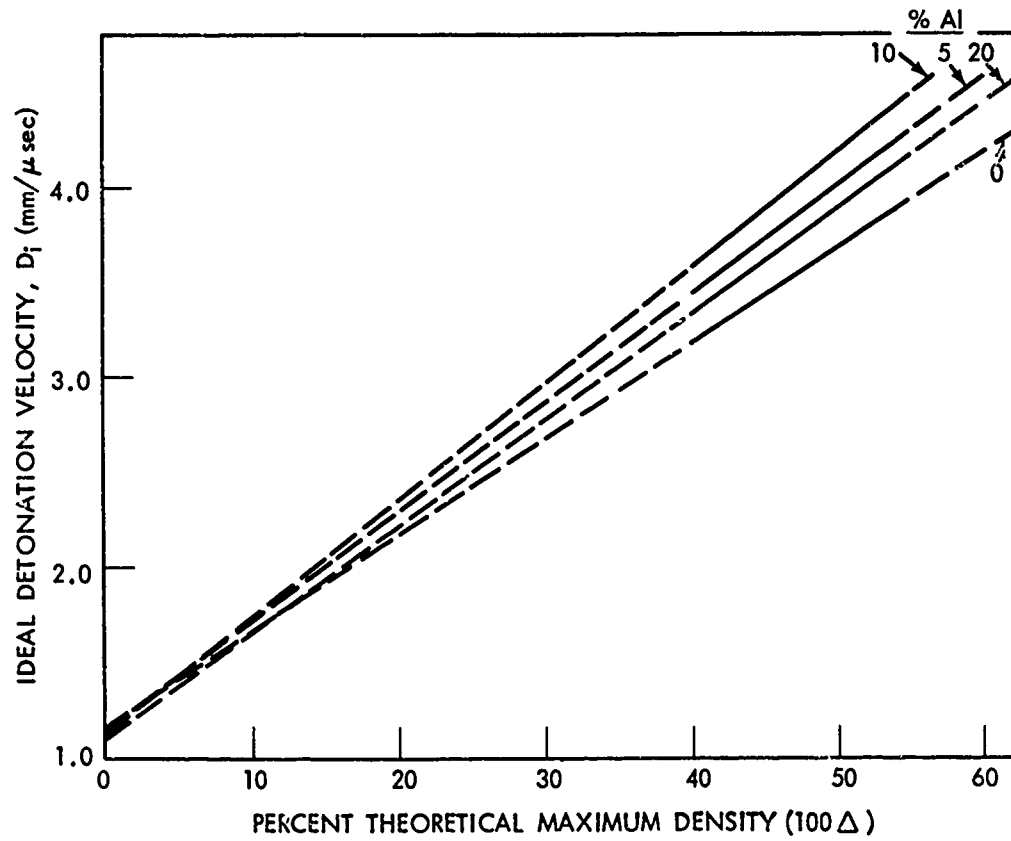
Effect of Al on  $D_1$ . The infinite diameter detonation velocity of pure AP is given<sup>3</sup> by

$$D_1 = 1.15 + 5.05 \Delta \quad (19)$$

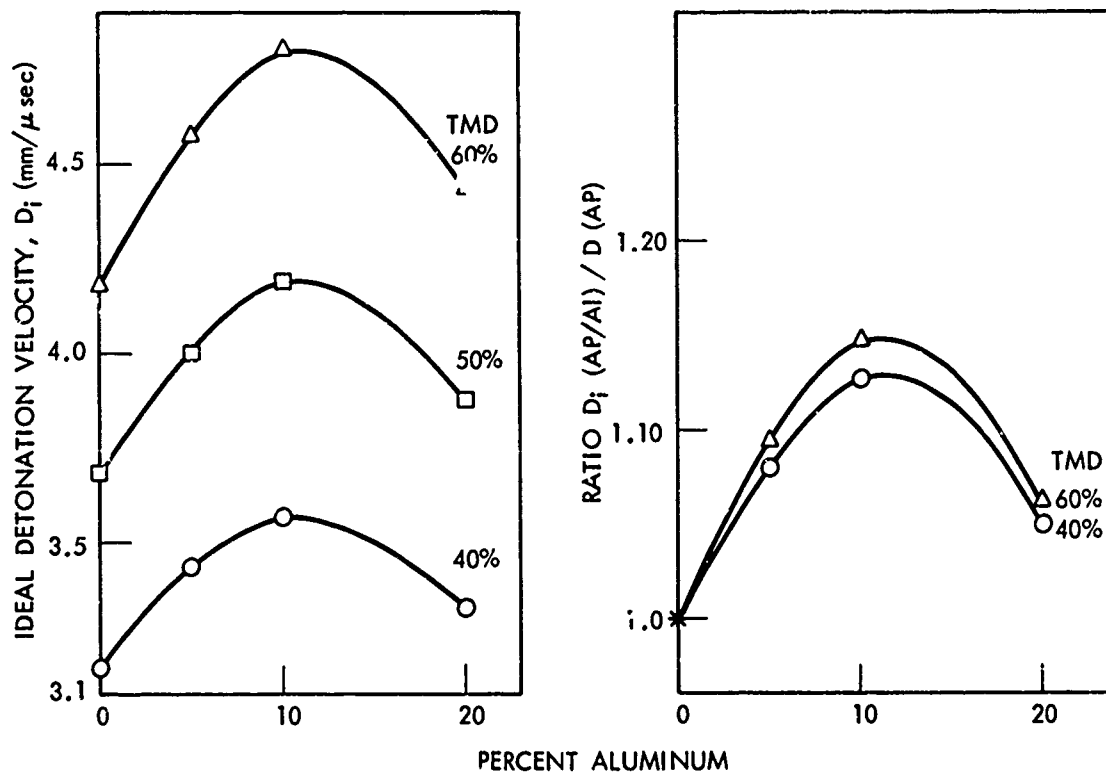
Eqs. (3), (14), (16) and (19) are used to illustrate in Fig. 12 the effect on  $D_1$  of adding Al to AP. The effect of Al on  $D_1$  gives a pattern of curves strikingly similar to that resulting from the diameter effect; compare Figs. 9 and 12a. As Fig. 12b shows, the added Al increases  $D_1$  up to a maximum at about 10% Al; the increase was 9% at 55% TMD. This differs from effects found with waxed AP. Instead of the fan pattern of Fig. 12a, the  $D_1$  curves for AP/wax paralleled the  $D_1$  curve for pure AP; their maximum increase occurred at about 20% wax and amounted to about 24% at 55% TMD.

To the authors' knowledge, there are no exactly comparable data for aluminized organic explosives except for a single point comparison between TNT and TNT/Al, 67.8/32.2 ( $D_1$  given in Appendix B). However, Coleburn et al<sup>7</sup> have studied the effect of Al on the detonation velocity at a fixed dia (50.8 mm) of TNT, RDX, and TNETB. Their results are tabulated in Appendix C and those for TNT/Al are illustrated in Fig. 13. The trend found with 51 mm dia charges should be the same as that which would be found with  $D_1$  although the velocities in the former case will be less than  $D_1$  values. The pattern of Fig. 13a is very like that of Fig. 10, i.e., decreasing  $d$  (increasing  $u$ ) or increasing % Al decreases  $D$ ; the  $D$ - $\Delta$  curves fan out from a point at high  $\Delta$  (here  $\Delta_0 \sim 1$ ). For TNT/Al,  $a_0$  and  $b_0$  are linear functions of % Al (See Appendix C); for AP/Al,  $b_0$  is nearly a linear function of % Al in the range 0 - 10%.

Aluminum in organic H.E. decreases  $D$ ; the greater the % Al and the lower the  $\Delta$  value, the greater the percentage decreases, as shown in Fig. 13b. As remarked above, Al increases  $D$  of AP (up to



(a)  $D$  VS  $\Delta$  CURVES



(b)  $D_i$  AND RELATIVE RATE VS % Al

FIG. 12 EFFECT OF Al ON  $D_i$  OF AP/Al

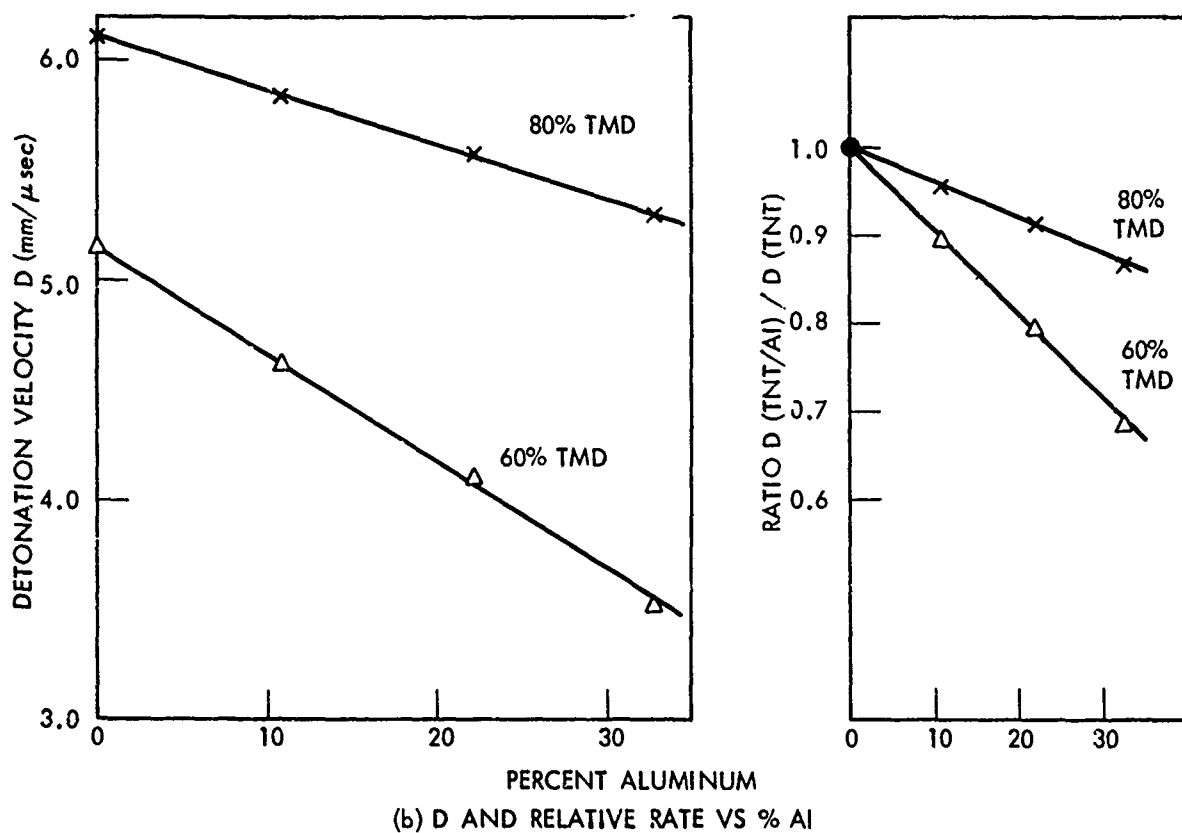
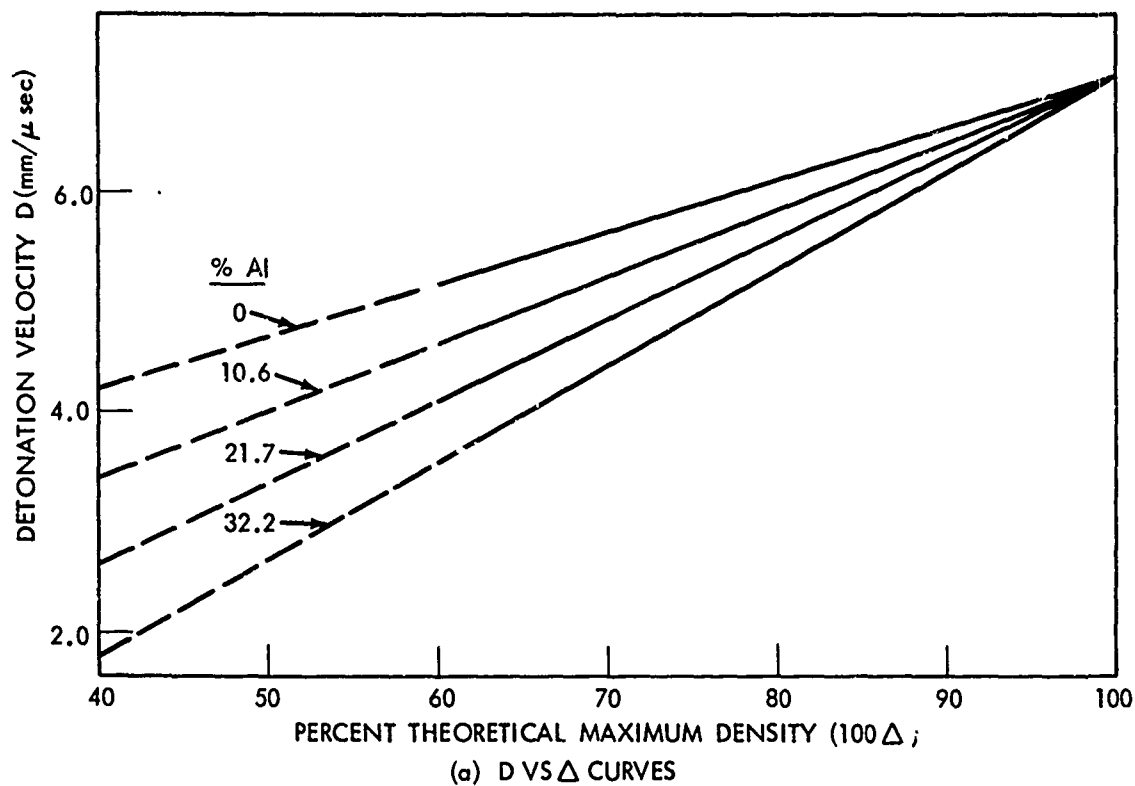


FIG. 13 EFFECT OF ALUMINUM ON DETONATION VELOCITY ( $d = 51$  mm) of TNT



a limiting content) and the percentage increase is greater at the higher  $\Delta$  value.

### Detonability and Shock Sensitivity

Table 1 contains data from which a detonability curve (critical dia  $d_c$  vs % TMD) can be constructed for AP/Al, 95/5. That curve is shown in Fig. 14 which also includes the analogous curves of  $10\mu$  AP<sup>1</sup> and of  $25\mu$  AP/wax, 90/10, for comparison. Note that Shot 927 has been plotted as a detonation only because the reaction of the charge was sufficient to initiate a pentolite witness; because the electronic instrumentation failed on this shot, there was no photographic record.

The work ended before a detonability curve for AP/Al, 90/10, had been run. However, one point on it was determined (See Table 3) and is shown in Fig. 14. Since the curve for 95/5 follows the form of that for 100/0 so closely, it seems reasonable to assume that that for 90/10 would follow that for 95/5 equally closely. It is evident that addition of Al has its greatest effect on lowering  $d_c$  at low  $\Delta$ ; this is the reverse of its effect on increasing  $D_1$  (See Fig. 12). Finally, Al seems far less effective than wax in decreasing  $d_c$  of AP.

The first large scale gap test was run on a series of AP/Al, 95/5 and the results are given in Table 7. They have not been plotted because they seem inconsistent with other gap sensitivity curves obtained for AP and AP/wax. Thus results at 40 and 55% TMD show that addition of 5% Al has increased the shock sensitivity of the  $9\mu$  AP to about that of the  $25\mu$  AP, but not to the value of  $25\mu$  AP/wax, 90/10. The few shots at 84.8% TMD and above show that the  $\Delta$  limit of shock induced reaction in the gap test has been shifted to higher  $\Delta$ , slightly beyond that of  $25\mu$  AP(0.844) and far short of that of  $25\mu$  AP/wax, 90/10(0.918). These data alone do produce a consistent picture of a shock sensitivity curve ( $P_g$  vs % TMD) for AP/Al, 95/5, similar in form and slightly below the curve for pure AP of the same particle size. This is the same effect, though of smaller magnitude, as that produced by adding wax to AP. But the gap test values at 67% and 80% TMD contradict the above results in that they show a decrease in

NOLTR 72-15

TABLE 7

GAP TEST RESULTS ON AP-144/A1-H5, 95/5

Density $\rho_0$ g/cc	% TMD	50% Point		Comment
		No.Cards	Pg kbar	
				All tests run with 50/50 1.56 g/cc pentolite booster
0.791	40.0	217	14.7	Modified test, Comp B witness
1.087	55.0	197	17.8	" " " " "
1.324	67.0	132	38.0	Regular test
1.582	80.0	76	66.0	" "
1.677	84.8	25<N<40	93<N<114	" "
1.685	85.0	0<N<50	*	" "
1.70	86.0	0	**	Regular and modified tests

\* Positive at zero cards, negative at 50.

\*\* Negative at zero cards.

AP N144 (9.3 $\mu$ )

A1 H5 (7 $\mu$ )

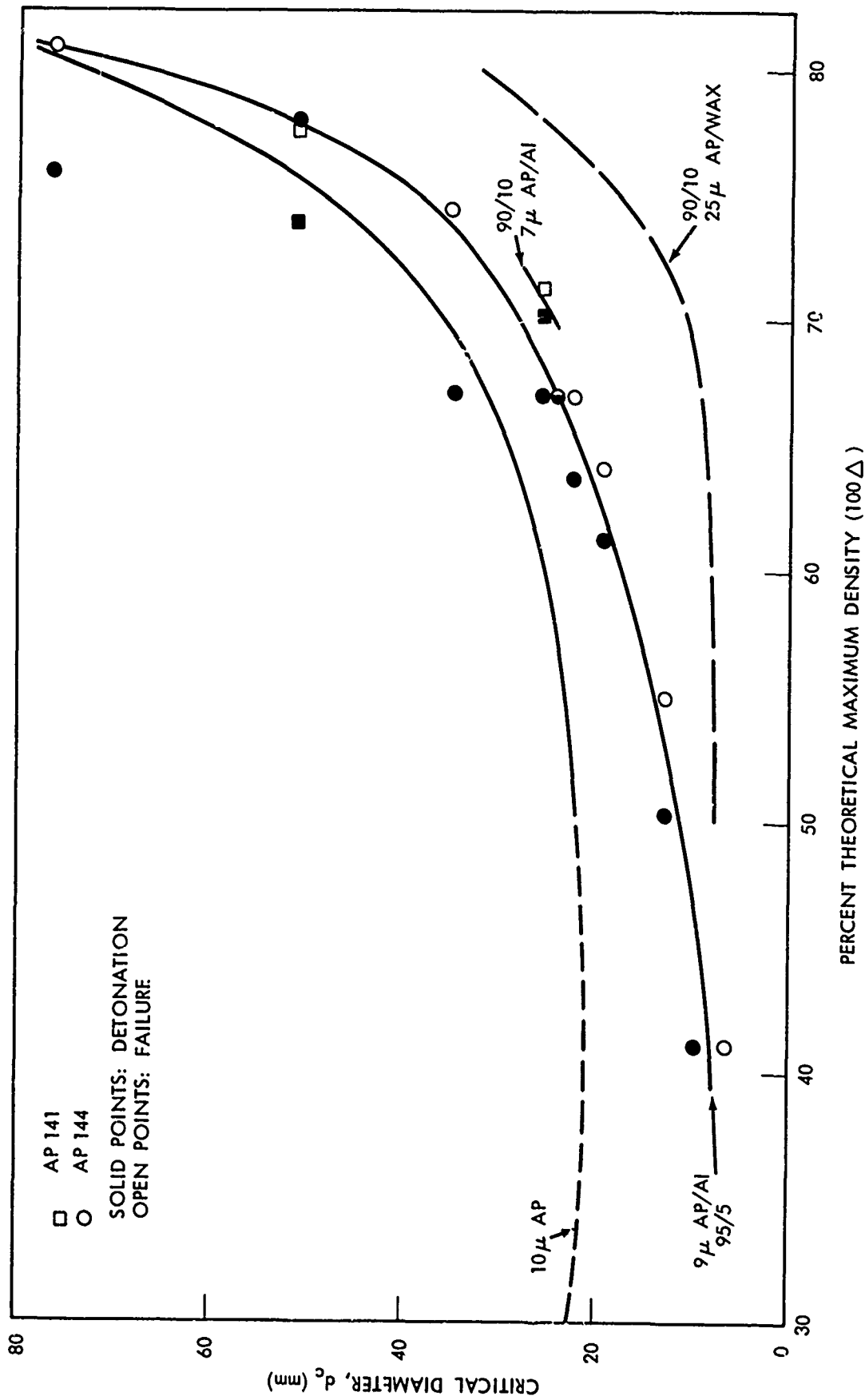


FIG. 14 DETONABILITY OF AP/AI MIXTURE

sensitivity caused by adding 5% Al. Thus the data of Table 7 would produce a shock sensitivity curve for AP/Al, 95/5, which crosses the AP curve twice, i.e., indicates increased sensitivity at high and low  $\Delta$ , decreased sensitivity at intermediate values. Because this complex sensitivity effect has not previously been found during years of gap testing, the results shown in Table 7 are unacceptable until they are confirmed or corrected by additional study.

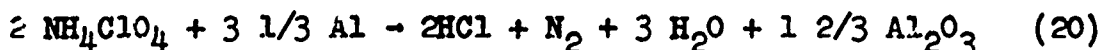
### Chemical Considerations

No equilibrium computations have yet been carried out with the Ruby code for the system AP/Al, but a number have been made on related systems and with propellant codes. For example, a typical propellant is AP/Al/ca.(CH<sub>2</sub>)<sub>n</sub>, 75/15/10. At 1000 psi and essentially voidless density this has a flame temperature ( $T_f$ ) of 3537°K and 98.3% of the Al in the products appears as Al<sub>2</sub>O<sub>3</sub>.<sup>11</sup> A comparable propellant of AP/Al/PBAA, 69/15/16, was used in the Ruby code at voidless density and with the assumption of complete reaction of the Al; the detonation temperature computed was  $T_j = 3198^\circ\text{K}$  and 97.5% of the Al appeared as Al<sub>2</sub>O<sub>3</sub>.<sup>12</sup> Hence for complete reaction of Al in a voidless solid,  $T_f$  seems to be a good approximation of  $T_j$  and the major aluminum product is Al<sub>2</sub>O<sub>3</sub>. The propellant code shows HCl as a major product; at approximately the same  $T$ , but at detonation pressure, the Ruby code shows Cl as a major product for the voidless charge.

For AP/wax, 90/10, nearly a stoichiometric mixture, it was found that  $T_f$  approximated the Ruby value of  $T_j$  better at 50% than at 80% TMD; for pure AP, the approximation was acceptable only in the vicinity of 50% TMD.<sup>3</sup> Since AP and its mixtures show regular detonation behavior (i.e., linear  $D$  vs  $\Delta$ ) only at 40-55% TMD, this is no great restriction. Moreover, at 50% TMD, the major Cl product shown by Ruby was HCl as was also the case for deflagration in the propellant code.

From this general information, it seems likely that  $T_f$  computed on a propellant code will furnish a good estimate of  $T_j$  computed on the Ruby code at  $\Delta \sim 0.5$ , and that the atomic ratio Al/O for the

mixture might be a good index of composition and performance of the AP/Al mixtures. Both of these assumptions are made for a complete reaction of the aluminum. The stoichiometric mixture would be 27.7% Al (Al/O of 0.4125) and the equation for the assumed reaction



The heat of reaction is then 2280 cal/g; the gas products, 18.42 moles/kg.

The Ruby code (with its current library and equation of state) has been notoriously unsuccessful in computing the detonation properties of AP. However, if the Ruby results are used in a relative fashion e.g., (computed parameter of mix)/(computed parameter of base material), they seem to give reasonable relative values. Thus in the case of AP/wax (25 $\mu$  AP, 125 $\mu$  wax), they indicated that only about half of the wax was reacting in the detonation.<sup>3</sup> Finger et al<sup>13</sup> have used the Ruby code for computing relative energies (available for moving the metal wall in the cylinder test) of HMX/perchlorate/hydrocarbon/Al systems relative to HMX. For the non-aluminized system, their results indicated complete reaction of 6 $\mu$  AP in the two inch dia test, the expected particle size effect on reaction time of perchlorates (3 $\mu$  KP 90%- and 44 $\mu$  KP 30% reacted in 0.5  $\mu$ sec), and the fact that reaction of the Al is post-detonation, e.g., 15% of the aluminum present had reacted after 4  $\mu$ sec. It seems evident from these results that sufficiently fine AP/HMX mixtures can exhibit detonation velocities enhanced by the AP/fuel reaction despite the fact that reaction depends on diffusion. It also seems evident that even fine Al, say 5 $\mu$ , cannot be expected to react rapidly enough to contribute to the detonation front of organic explosives.

The present results indicate, however, that some reaction must occur between the Al and the AP in time to contribute to the detonation front. Although the effects of Al on decreasing  $d_c$  and  $P_g$  of AP could be explained qualitatively on the basis of physical phenomena alone, it is hard to see how the observed increase in D could be obtained without a chemical reaction. For the purpose of studying the results

---

\*Fluorinated in some cases.

at relatively high porosity (40-50% TMD), the arbitrary mechanism of Eq. (20) will be used. This converts all Al to  $\text{Al}_2\text{O}_3$  (solid or liquid), all Cl to HCl and the remainder of H to  $\text{H}_2\text{O}$ . As Table 8 shows, the products of deflagration are as well approximated in this fashion as were those of AP/wax, 90/10, at 59% TMD.<sup>3</sup>

Prediction of D. Kamlet<sup>14</sup> has devised a simple calculation which closely approximates the values computed in the Ruby code for most organic (C-H-N-O) H. E. at 50-100% TMD. His expression for detonation velocity is

$$D = n^{\frac{1}{2}} M^{\frac{1}{4}} Q^{\frac{1}{4}} (1.01 + 1.31 \rho_v) \quad \text{or}$$

$$D = n^{\frac{1}{2}} M^{\frac{1}{4}} Q^{\frac{1}{4}} (1.01 + 1.31 \rho_v \Delta) \quad (21)$$

where D is in mm/ $\mu\text{sec}$ , n is number of moles of gas product/g H.E., M is average molecular weight of the gas products, Q is heat of reaction in cal/g H.E., and  $\rho_v$  is the voidless density of the H.E. Since  $nM \approx (\text{mass gas products})/(\text{mass H.E.})$ ,

$$nM = 1-x$$

where x is the mass fraction of condensed products. Hence Eq. (21) can be written

$$D = [nQ (1-x)]^{\frac{1}{4}} (1.01 + 1.31 \rho_v \Delta) \quad (22)$$

Eq. (22) displays a bit more obviously than (21) the effect of decreasing n while increasing Q and x, as reaction with Al would do.

Because Eq. (22) approximates values computed on the Ruby code, it is of little use in estimating the absolute value of D of AP. However, for 90/10, AP/wax, the ratio  $D(\text{waxed AP})/D(\text{AP})^*$  at 50% TMD is 1.27 by Eq. (22) and 1.25 by Ruby. [The ratio of the experimental  $D_1$  values was 1.26 for the 80/20 mixture; hence the estimate of about half the wax reacting.] The question now arises as to whether Eq. (22)

---

\*4.41 mm/ $\mu\text{sec}$ . Arbitrary decomposition for detonation of AP at 50-100% TMD has  $\text{Cl}_2$  as product.<sup>1</sup>

TABLE 8

COMPUTED PARAMETERS FOR DEFLAGRATION OF AP/Al, 90/10

Products*	Moles/kg	Arbitrary
H <sub>2</sub> O	11.506	11.489
Al <sub>2</sub> O <sub>3</sub>	1.848**	1.850
HCl	6.441	7.660
Cl	1.125	0
Cl <sub>2</sub>	0.039	0
O <sub>2</sub>	5.991	6.800
O	0.146	0
HO	0.927	0
HO <sub>2</sub>	0.004	0
H <sub>2</sub>	0.113	0
H	0.029	0
AlCl <sub>3</sub>	0.002	0
AlCl <sub>2</sub>	0.002	0
AlOCl	0.005	0
N <sub>2</sub>	3.570	3.830
NO	0.520	0
<hr/> n 30.41 Q 797.9 T 2933°K		<hr/> 29.78 moles/kg 1032 cal/g --

\* P<sub>c</sub>=1000 psi. Also considered and present in concentrations <10<sup>-3</sup> mole/kg: NH, AlHO<sub>2</sub>, Al<sub>2</sub>O, AlCl, NH<sub>2</sub>, Al, AlN, O<sub>3</sub>, AlO, AlH, N<sub>2</sub>H<sub>4</sub>, N, NH<sub>3</sub>, and Al<sub>2</sub>O<sub>2</sub>.

\*\* Liquid.

can be used in the same way for AP/Al. It should be noted that the oxidation products from wax are  $H_2O$ ,  $CO$ , and  $CO_2$ ; these are also normal detonation products of H.E. whereas  $Al_2O_3$  is not.

The first step is to try application of Eq. (22) to lightly aluminized mixtures of organic H.E. This is done for TNT and RDX in Table 9. The calculated values indicate that addition of Al to organic H.E. should decrease  $D$ , as indeed it does (see Appendix C). Moreover, the decrease is exactly the same whether the Al reacts or is completely inert. [In the case of no reaction of finely divided Al, the metal should act as an energy sink by entrainment and by heat adsorption. No attempt was made to estimate these effects.] Comparison of the calculated ratio  $D(HE/Al)/D(HE)$  with the experimental values at 90 and 50% TMD shows that agreement is fair at  $\Delta = 0.9$  and poor at the lower density. This probably demonstrates the inadequacy of the second factor of Eq. (22) in representing the strong effect of  $\Delta$  on  $D$  for aluminized organic H.E. It does not contradict (or establish) the suggested dependence of  $D$  on  $n$ ,  $Q$ , and  $X$ .

Table 10 contains the analogous computations for the series AP/Al as well as the corresponding ratio values produced by the experimental results (Fig. 12). It is evident that the density effect on the ratio values is small,  $0.4 \leq \Delta \leq 0.55$ , and that the use of Eq. (22) to compute the ratios produces a density effect comparable in size and sign to those observed experimentally. The trend of the calculated and experimental values are the same, as Fig. 15 shows. The fact that the latter are below the calculated is to be expected for a number of reasons: AP has a low detonation temperature, Al has a high vaporization temperature, and Al of  $5\mu$  size reacts slowly in terms of detonation phenomena. It seems likely that such oxidation/reduction reaction as did occur took place on the surface of the Al particles and extended only to the depth of a layer which had been heated sufficiently to react with the available oxygen. Even for the smallest amount of Al (5%), all of the Al was not available to react in time to contribute to the detonation velocity. This qualitative information and similar trends of the curves of Fig. 15 suggest that



TABLE 9

COMPARISON OF RATIOS COMPUTED FROM EQ(22) WITH EXPERIMENTAL VALUES  
(Aluminized Organic H. E.)

Al/O	Material	$\rho_v$ g/cc	$10^3 n^*$ moles/g	$Q^*$ cal/g	$(1-x)$	$nQ(1-x)$	$[nQ( )]^{1/4}$	2nd Factor	RATIOS $D_{HE}/A1/-$ $\frac{D_{H.E.}}{A=0.9 \quad A=0.5}$	
									1	1
0	TNT	1.654	25.3	1282	0.721	23.4	2.20	(1.01+2.17A)	1	1
0.170	TNT/Al 89.4/10.6	1.72	19.7	1655	0.516	16.8	2.03	(1.01+2.25A)	0.945	0.940
"	" **		22.5	1147	0.644	16.7	2.02	"	0.940	0.936
"	Experimental***								0.99	0.91
0	RDX	1.802	33.8	1482	0.919	46.0	2.60	(1.01+2.36A)	1	1
0.153	RDX/Al 90/10	1.86	27.6	1813	0.693	34.7	2.43	(1.01+2.44A)	0.956	0.952
"	" **		30.4	1334	0.827	33.5	2.41	"	0.948	0.944
"	Experimental***								0.97	0.78

NOLTR 72-15

\* O used to form  $Al_2O_3$ ,  $H_2O$ ,  $CO_2$  in sequence  
 \*\* No reaction of Al  
 \*\*\* Appendix C

TABLE 10

## COMPARISON OF RATIOS COMPUTED FROM EQ (22) WITH EXPERIMENTAL VALUES

(Aluminized AP)

AP/Al %Al	Al/O	$\rho_v$ g/cc	$10^3 n$ moles/g	$Q$ cal/g	(1-x)	nQ(1-x)	First Factor Eq(22)	Second Factor Eq(22)	Computed Ratios $D(AP/Al)/D(AP)$	
									$\Delta=0.40$	$\Delta=0.55$
0	0	1.950	34.04	405	1	13.77	1.93	(1.01+2.55A)	1	1
5	0.0573	1.977	32.97	678	0.906	20.24	2.12	(1.01+2.59A)	1.11	1.11
10	0.121	2.006	29.78	1032	0.811	24.92	2.23	(1.01+2.63A)	1.17	1.18
10*	0.121	2.006	32.55	292	0.900	8.55	1.71	(1.01+2.63A)	0.90	0.91
15	0.192	2.035	26.58	1388	0.717	26.45	2.27	(1.01+2.67A)	1.20	1.21
20	0.272	2.065	23.38	1740	0.622	25.33	2.24	(1.01+2.70A)	1.19	1.20
23	0.325	2.083	21.46	1955	0.566	23.74	2.21	(1.01+2.73A)	1.19	1.19
27.7	0.412	2.113	18.42	2280	0.478	20.07	2.12	(1.01+2.77A)	1.14	1.15

NOLTR 72-15

Experimental  
Ratios\*\*

%Al	Experimental Ratios**
0	1.0
5	1.08
10	1.13
20	1.05
	1.06

\* No reaction but AP/Al arbitrary mechanism used, not that for AP alone<sup>1</sup>.

\*\* Fig. 12a

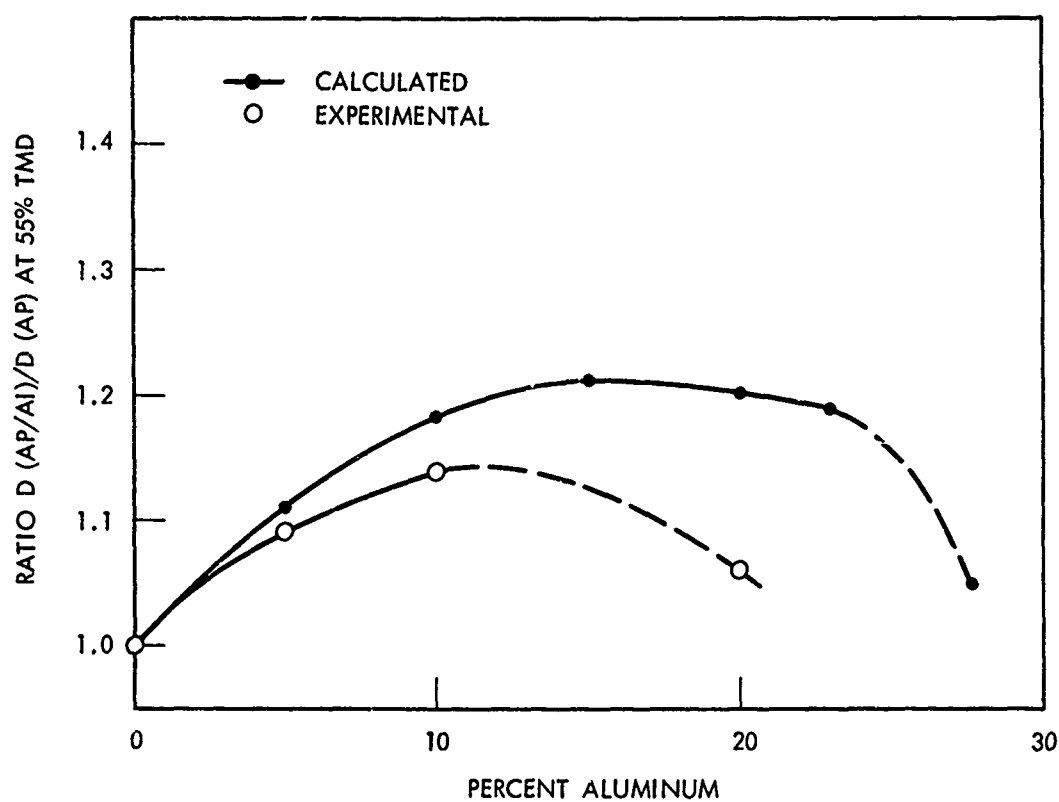


FIG. 15 EFFECT OF ALUMINUM ON DETONATION VELOCITY OF AP

Eq. (22) and the arbitrary reaction mechanism chosen do give guidance in the relative effects to be expected from aluminized AP for reaction of all Al present.\* In particular, and in contrast to AP/wax, the computations of Fig. 15 show the maximum increase in D at about 15% Al (Al/O of 0.192) instead of at the stoichiometric concentration. In other words, the effect on D of decreasing the volume of gas products is more than offset by the increase in chemical energy up to 15% Al. At no point, however, will AP/Al be as effective as AP/wax although the temperature of the products (for complete reaction) is

-----  
 \*Use of this method of prediction must be restricted to  $\Delta \sim 0.5$  and mixtures of finely divided components for several reasons. This is the region in which the results show regular detonation behavior and, therefore, the one most favorable for good comparisons. Then the detonation pressure, temperature, and hence reaction products will probably differ at different compactions. Thus, AP alone seems to form  $\text{Cl}_2$  at all practical densities for detonation<sup>2</sup> but AP/wax seems to form HCl at low  $\Delta$ ,  $\text{Cl}_2$  (or Cl) at high  $\Delta$ <sup>3</sup>. Second, it is difficult to obtain an acceptable comparison of predictions made with total consumption of the fuel to results obtained with only partial consumption. Finally, the present method seems to check out at  $\Delta \sim 0.5$  but does not reproduce the relative trends over any range. For example, in  $D_1 = a_0 + b_0 \Delta$ , for increasing percentage of fuel:

<u>Material</u>	<u>Experimental results</u>	<u>Present method of Prediction</u>
Org. H.E./Al	$a_0$ decreases, $b_0$ <u>increases</u>	$a_0$ decreases $b_0$ <u>decreases</u>
AP/wax	$a_0$ increases, $b_0$ <u>approx. const</u>	$a_0$ increases $b_0$ <u>increases</u>
AP/Al	$a_0$ <u>approx. const</u> $b_0$ increases	$a_0$ <u>increases</u> $b_0$ increases

-----

somewhat higher for AP/Al. In a 3-component mixture wax could be used to maintain the volume of the gaseous products and Al to increase their temperature. It is possible that with the volatile fuel to raise the temperature more rapidly, a greater portion of the aluminum could react in time to contribute to the detonation front.

Eyring Reaction Zone Length. The Eyring reaction zone length  $z$  is defined,<sup>15</sup> in our present notation, as

$$z = -\beta/D_1 \quad (23)$$

Hence over the range of regular behavior (i.e.,  $\Delta \leq 0.55$ ), Eqs. (23) and (11) give

$$z = -(a' + b'\Delta)/(a_0 + b_0\Delta) \quad (24)$$

As in the case of Ruby code results, relative values of  $z$  are preferred because the absolute values have not been shown to have physical significance and also because the relative values should be the same for either the Eyring curved front treatment or the Wood and Kirkwood<sup>16</sup> modification of it. Table 11 contains the relevant data for AP/Al mixtures and values of  $z$  at  $\Delta = 0.4$  and  $\Delta = 0.55$ , the limits of the range of regular behavior for these mixtures. [The lower limit is imposed here because of the difficulty in preparing acceptable charges at lower  $\Delta$  with the state of subdivision of the present components.]

At the lower  $\Delta$  limit, the  $z$  value is approximately the same for every composition except AP/Al, 90/10; in this case, it is 75% smaller. At the upper  $\Delta$  limit, both the 90/10 and the 95/5 mixes show  $z$  values greater than that of AP. This results, in part, from the fact that AP shows a decrease in  $z$  with increasing  $\Delta$  over the range of regular behavior whereas the 95/5 and 90/10 mixes show an increase. Interestingly enough, the trend for pure AP is inconsistent\* with its detonability curve; although it does show Group 1 detonability at lower  $\Delta$ ,

---

\*This assumes linear variation of  $z$  with  $d_c$ .

TABLE 11

## EFFECT OF ALUMINUM ON EYRING REACTION ZONE LENGTH OF AP

Material	$a_0$	$b_0$	$a'$	$b'$	Eyring Reaction Zone Length $z$ (mm)	
					$\Delta=0.4$	$\Delta=0.55$
AP(N141)	1.15	5.05	-9.14*	-6.09*	3.6	3.2
AP/A1 95/5	1.13	5.73	-0.99	-30.67	3.9	4.2
AP/A1 90/10	1.13	6.11	7.76	-43.7	2.7	3.6
AP/A1 80/20	1.10	5.57	-10.3	-4.6	3.6	3.1

\* Derived from D- $\Delta$  relations for  $d = 50.8$  mm and for  $d = \infty$ .

it has a Group 2 trend in this range. The 80/20, AP/Al and pure AP show the same  $z$  values; this fact suggests a balance between the heat produced by the fraction of aluminum that is reacting and the heat lost to the remaining Al that is inert. The increase in  $z$  with increase in  $\Delta$  for the 95/5 and 90/10 mixes is consistent with their detonability trends (Fig. 14) and suggests that the diffusion reaction is favored by low  $\Delta$ . In this particular case, it may be; it depends not on diffusion mixing of two gases, but on diffusion of  $O_2$  to a heated surface of the Al particles. Detonation temperature and hence depth of heated layer may increase with decreasing  $\Delta$ .

Finally, the  $z$  values of  $7\mu$  AP relative to those of TNT at 55% TMD are about the same<sup>u.t.</sup> for the TNT used by Stesik and Akimova<sup>4</sup> and about three times those found for the unconfined TNT charges used by Urizar et al.<sup>8</sup> As we have already seen for AP<sup>1</sup>, the state of subdivision has a large effect on  $z$ ,  $a'$  and  $b'$ .

#### SUMMARY

Mixtures of  $7\mu$  Al with 7-9% AP exhibit Group 2 behavior, as does pure AP. Over the range of 55 to 40% TMD (and possibly lower) they exhibit regular detonation behavior, i.e., show a linear dependence of  $D$  on  $\Delta$  at  $d > 25$  mm and a linear dependence of  $D$  on  $u$  at fixed  $\Delta$ . [Beyond this range, at  $\Delta > 0.55$ , the  $D$  vs  $\Delta$  curves exhibit a maximum before reaching the critical  $\Delta$ .]

AP/Al  $D$  vs  $\Delta$  curves extrapolated from the regular range intersect at low  $\Delta$  (here, near zero). The pattern is a fan of curves from  $\Delta \sim 0$  with slopes a linear function of  $d^{-1} \equiv u$ . Organic H.E./Al show a fan of curves from a high  $\Delta$  ( $\sim 1$ ) with slopes a linear function of  $u$ .

Addition of 5-10% Al to AP increases  $D_i$ ; addition of any Al to organic H.E. lowers  $D_i$ . The patterns ( $D$  vs  $\Delta$ ) for varying Al content are very similar to those found in the diameter effect in that AP/Al curves fan out from  $\Delta \sim 0$  and organic H.E./Al curves, from  $\Delta \sim 1$ .

Increasing the particle size of either AP or Al decreased the D measured at a given u and  $\Delta$ . Change in the size of the oxidizer had more effect than change in the size of Al.

Aluminized AP exhibited greater detonability than pure AP. The effect on the shock sensitivity of adding Al to AP was not adequately established in this study.

An arbitrary mechanism for the reaction of AP/Al at  $\Delta \sim 0.50$  was devised. This was used in conjunction with Kamlet's method of calculation in lieu of the Ruby code. The relative results,  $D(\text{AP/Al})/D(\text{AP})$ , differed from the experimental results in the manner to be expected for partial reaction of the Al. The maximum increase in  $D_1$  observed was at 10% Al; that predicted was ca. 15% Al.



REFERENCES

1. D. Price, A. R. Clairmont, Jr., and I. Jaffe, "Explosive Behavior of Ammonium Perchlorate", Combust. Flame 11, 415-25 (1967). See also NOLTR 67-112.
2. D. Price, A. R. Clairmont, Jr., J. O. Erkman, and D. J. Edwards, "Infinite Diameter Detonation Velocities of Ammonium Perchlorate", Combust. Flame 13, 104 (1969). See also NOLTR 68-182.
3. D. Price, A. R. Clairmont, Jr., and J. O. Erkman, "Explosive Behavior of a Simple Composite Propellant Model", Combust. Flame, 17(3), 323 (1971). See also NOLTR 69-16.
4. D. Price, "Contrasting Patterns in the Behavior of High Explosives," Eleventh Symposium (International) on Combustion, p. 693. The Combustion Institute: Pittsburgh (1967).
5. J. O. Erkman and D. Price, "Comparison of Curvature of Detonation Front in AP with that Found in Some Conventional Explosives", NOLTR 69-235, 25 May 1970.
6. L. A. Roslund and N. L. Coleburn, "Hydrodynamic Behavior and Equation-of-State of Detonation Products Below the Chapman-Jouquet State", Preprints of the Fifth Symposium on Detonation, ONR Report DR-163, p. 405, Aug 1970.
7. N. L. Coleburn, NOL, private communication.
8. M. J. Urizar, E. James, Jr., and L. C. Smith, "Detonation Velocity of Pressed TNT", Phys. Fluids 4, 262, (1961).
9. R. D. Cowan and W. Fickett, "Calculation of the Detonation Properties of Solid Explosives with the Kistiakowsky-Wilson Equation of State", J. Chem. Phys. 24, 932 (1956).
10. D. Price, A. R. Clairmont, Jr., J. O. Erkman, and D. J. Edwards, "Ideal Detonation Velocity of Ammonium Perchlorate and Its Mixtures with H.E.", NOLTR 68-182, 16 Dec 1968.
11. L. J. Gordon and H. E. Boerlin, "A Practical Approach to Computer Programming for Specific Impulse Calculations", in Kinetics, Equilibria and Performance of High Temperature Systems (edited by G. S. Bahn and E. E. Zukoski), Butterworths (Washington) 1960, pp. 152-165.

REFERENCES

12. R. F. Chaiken, "Comments on the Ruby Code", App. II of Vol. II of Project Sophy - Solid Propellant Hazards Program, AFRPL - TR 67-211, Aug 1967.
13. M. Finger, H. C. Hornig, E. L. Lee, and J. W. Kury, "Metal Acceleration by Composite Explosives", Reprints of the Fifth Symposium (International) on Detonation, ONR Report DR-163, Aug 1970, pp. 55-67.
14. M. J. Kamlet and S. J. Jacobs, "Chemistry of Detonation. I. A Simple Method for Calculating Detonation Properties of C-H-N-O Explosives", J. Chem. Phys. 48, (1) 23, (1968).
15. H. Eyring, R. E. Powell, G. H. Duffy, and R. B. Parlin, "The Stability of Detonation", Chem. Rev. 45, 69 (1969).
16. W. W. Wood and J. G. Kirkwood, "Diameter Effect in Condensed Explosives. The Relation Between Velocity and Radius of Curvature of the Detonation Wave", J. Chem. Phys. 22, 1920 (1954).

## Appendix A

## Dry Blending Of Mixtures Containing AP

Our initial mixtures for propellant models were made with 25 $\mu$  ammonium perchlorate (AP). As soon as finer AP (~9 $\mu$ ) was used, the mixes no longer appeared uniform but contained agglomerates of up to 5 mm in diameter. This difficulty was encountered first in AP/H.E. mixtures and then in AP/Al. Subsequent analyses of the larger clumps in the AP/Al mixes showed an Al content of 12% to 16% although the overall composition of the preparation was 10% Al. Hence, the agglomeration resulted in non-uniformity in both chemical composition and particle size.

At first it was assumed that the tendency to form agglomerates was caused chiefly by the AP's moisture pick-up. It can certainly be demonstrated that this will cause clumping, but so too will handling the fine AP in a moisture free atmosphere. Thus, tumbling 200 g AP-N139 (8.8 $\mu$ ) for five minutes in a twin shell blender converted it into spherical aggregates, many larger than 2.4 mm in diameter. When eight golf balls were used to mill the AP during tumbling, both the size and number of the aggregates were reduced. The weight percent distribution after tumbling was:

<u>Material</u>	<u>&gt;2.38 mm</u>	<u>&gt;0.84 mm</u>	<u>&lt;0.84 mm</u>
AP	40	36	24
AP & golf balls	20	40	39

Agglomeration of fine AP, despite its storage in moisture-vapor proof bags and subsequent handling in a dry box, indicates that cohesion between the small particles is a major factor in clump formation. It is also one which becomes more important as the particle size decreases. Subsequent confirmation of this view was found in a study of the behavior of zinc oxide powders by Meissner et al.\* The fine ZnO powder ( $\leq 0.25\mu$ ) seemed to duplicate the pelletizing in AP (~9 $\mu$ ); it was explained in terms of the action of van der Waals forces. Additional information on AP and AP mixes came from a study made by B. J. Alley and H. W. Dykes. In a classified report of the Army Missile Command in January 1967, they described a correlation between the difficulty of dispersion of the powders and the size of the difference between their dry and wet packing fraction. For example,

\*H. P. Meissner, A. S. Michaels, and R. Kaiser, I & EC Proc Des & Devel. 3 197 and 202 (1964).

## Packing Fractions (E) and Ease of Dispersion

Average Particle Size of AP powder, $\mu$	E, dry	E, wet	Dispersion
6	0.363	0.751	Great difficulty
20	0.530	0.738	Moderate difficulty
50	0.705	0.702	No difficulty

It is evident from these results that our fine AP ( $\sim 9\mu$ ) would be expected to give difficulty in dry mixing and that the most probable source of the difficulty is the agglomeration which occurs so rapidly.

Once agglomerates have formed, they persist as recognizable entities in the charge. For example, Figure 1 (Shot 720-still) shows a 1 g/cc AP charge prepared in the hydraulic press from the coarsest screen fraction from tumbling AP-N139, i.e., particles  $>2.4$  mm. To be sure, some of the agglomerates would be crushed under higher pressures (which would produce AP charges of higher %TMD that are difficult to impossible to detonate). However, the crushed agglomerates then appear as heterogeneous areas (specks) in the finished charges, as photographs below will illustrate. When clumps are evident in the powder, it is normal practice to roll the material and disperse lumps by crushing immediately prior to making the charge.

Because fine AP agglomerates so rapidly, successfully mixing it with another material such as Al powder depends on preventing clump formation, or breaking up any agglomerates formed, or both. It was shown by tumbling the fine ( $\sim 5\mu$ ) Al powder, that the Al alone did not form aggregates. However, AP/Al 90/10 or 95/5 agglomerated rapidly; it is reasonable to suppose that this results chiefly from the agglomeration of the AP. The fine Al serves to produce a gray charge on the surface of which aggregates of AP appear as contrasting white areas.

In studying the preparation of AP/Al mixtures only those that appeared uniform as a loose mix were isostatically pressed to prepare charges. Machining the pressed slug revealed the AP agglomerates. Figure 1b is a photograph of a control charge which was made by the routine charge preparation used for organic H.E. Obviously the routine must be modified to produce AP/Al charges satisfactory for the present study.

Although the preliminary results of dry mixing procedure coupled with milling were promising, it was not very attractive for processing large batches. Consequently an attempt was made to prepare mixes with a liquid carrier. Our limited experience with wet blending (using hexane or heptane as the fluid) indicated that the resulting product will be caked. Thus, we have to use a grinding operation to obtain fine material for producing low density charges which are essential in our research program. In no case did we



(a). CHARGE ( $\rho_o = 1 \text{ g/cc}$ ) PREPARED FROM COARSEST FRACTION OF TUMBLED AP, SHOT 720.



(b).  $9\mu \text{ AP}/5\mu \text{ Al}$ , 90/10, ROUTINE MIXING,  $\rho_o = 1.28 \text{ g/cc}$ . SHOT 614.

FIG. A1

produce charges superior to that of Figure 1b. In addition to that major drawback, wet blending also presents the problems of finding liquid carriers which are not solvents for any mixture component and of procuring mixing equipment suitable for slurries. For these reasons, all our propellant models having two or more ingredients have been produced by dry blending. Our experience with various methods of dry blending of AP/Al and AP/Wax/HMX is described in the following.

The tendency of AP to agglomerate so readily in dry mixtures has been attributed to several factors or mechanisms. One is the presence of "mother liquor", a residue of the solution from which the AP was precipitated.\* Another is the moisture which the AP picks up as it is handled; to offset caking attributed to this effect, 0.15% - 0.25% tricalcium phosphate\*\* (an anti-caking agent) is added to the fine AP when it is ground, and the material is handled in dry-boxes. Another suggested mechanism is that van der Waal forces between fine particles of AP cause the growth of aggregates as the material is handled and mixed. None of these causes of agglomerations has been proven or disproven in our work, but it seems obvious that some milling action must occur during the mixing process if agglomerates are to be eliminated.

A number of approaches have been tried for mixing AP based propellant models. These have been on a small scale, both for expediency (NOL has no equipment for large scale dry mixing) and for safety. Safety to personnel has also been assured by performing the experiments in the explosion chamber, or at a remote site. Because the equipment is relatively inexpensive, we have not been unduly concerned with its destruction. Although vigorous agitation has been used in some cases, we feel we have not come near the severe treatment which AP receives in the hammer mill when it is ground.

By examining the blended product while it is still a powder, we can determine if gross clumping of the AP has taken place. Small clumps can be more readily detected by pressing the powder in the isostatic press and machining the pressing (usually into the form of a cylindrical charge). Clumps of AP show as white spots on the surfaces of these charges. Each spot represents some cross section of a clump. We judge the adequacy of the blending by the number of spots, and by their size. Size of a spot can be determined conveniently by using a magnifier equipped with a reticle.

In discussing the various methods we have used for blending it is convenient to group them under two headings. The first group of methods uses mixers which depend on tumbling the ingredients and have no internal power-driven agitators. The tendency of AP to form clumps has been defeated (at least partially) by including golf balls or porcelain balls in the machines along with the ingredients.

\*In propellant grade AP this should be  $<0.02\%$   $H_2O$  and seems an unlikely cause.

\*\*J. A. Lovenger and T. L. Willetts in a classified report of Oct 1970 from Rohm and Haas Co., Huntsville, Ala. describe  $Al_2O_3-C$  (Degussa, Inc., N.Y.), a flow and anticaking agent of 0.005 - 0.030%, which seems much more effective than TCP.

The second group of methods of mixing uses equipment with driven internal agitators. These give the material a treatment similar to that encountered in the hammer mill. The Waring Blender (WB) and the Patterson-Kelly Twin Shell blender with an intensifier bar (TSIB) are included in this group.

Mixes of AP and aluminum and of AP/Wax/HMX have been prepared, using AP of about 25 $\mu$  and 7 $\mu$  average particle sizes. The following list describes the components and gives their abbreviations as used in the remainder of this section.

<u>Material</u>	<u>Average Particle Size, <math>\mu</math></u>	<u>Abbreviation</u>
AP-N-141	7	AP7
AP-N-142	25	AP25
Aluminum powder (H-5)	5	Al5
Carnauba Wax	~125	Wax
HMX 586-2	14	HMX

Mixers Depending on Tumbling. The following discussion on mixing is concerned with machines which have no driven internal agitators and therefore no bearings which are exposed to the mix. That is, the material is tumbled or shaken. The Patterson-Kelly Twin Shell (TS) blender is a well-known machine which tumbles the material. The drum or barrel blender also depends on tumbling. A somewhat different action is given the material by the paint shaker (as used in a typical paint store or paint shop). All of these machines require golf balls or porcelain balls in the mix to counteract the tendency of AP to agglomerate. Figure 3 shows a charge made from a 500 g mix of AP7/Al5, 90/10 prepared in the TS using nine golf balls and a run period of one hour. The white spots show that the AP formed some agglomerates despite the milling action of the golf balls. Sizes of the spots in the photograph can be estimated by noting the scales, each division being 0.5 inch.

A charge such as that shown in Figure 3, although it has fewer and smaller specks than that of Figure 1b, is still unsatisfactory for our use. Production of better mixes in the TS obviously calls for more intense milling action. This is accomplished by using porcelain balls 1.27 cm (0.5 in.) in diameter. The shell is stainless steel so there is some cause for concern when these balls impact a thin layer of mix on the metal surface. These materials are relatively insensitive, however, and we repeat that the fine AP is ground in a hammer mill. Hence, the operation was undertaken with a minimum of concern. Personnel were protected by placing the mixer in a remote location. Figure 4 shows two views of a charge made from a 500 g mix of AP7/Al5, 90/10, prepared in 20 minutes in the TS with

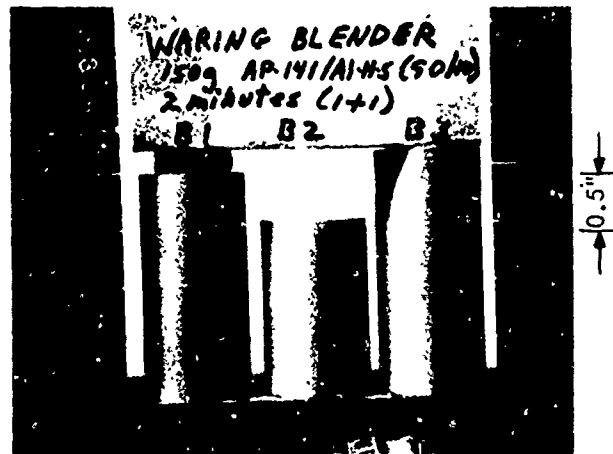


FIG. A2 AP( $\sim 7\mu$ )/Al ( $\sim 5\mu$ ), (90/10) PREPARED IN WARING BLENDER WITH PLASTIC BEADS.



FIG. A3 AP( $\sim 7\mu$ )/Al ( $\sim 5\mu$ ), (90/10) PREPARED IN TWIN SHELL BLENDER.



300 of the ceramic balls. A significant improvement has been made in the mix -- compare Figure 4 with Figure 3. The largest spot in Figure 4 has a dimension of about  $600\mu$  while the average is between 200 and  $300\mu$ . Equally good results were obtained by the same method when 1000 g of the mix and 600 ceramic balls were used. Compared to the golf ball method, we have doubled the batch size and reduced the mixing time by a factor of 3, resulting in an increase of production by a factor of 6, and have obtained a much better mix. Larger batches could be prepared by acquiring a larger machine; production models are available with capacities ranging from 1 to 2,000 cubic feet.

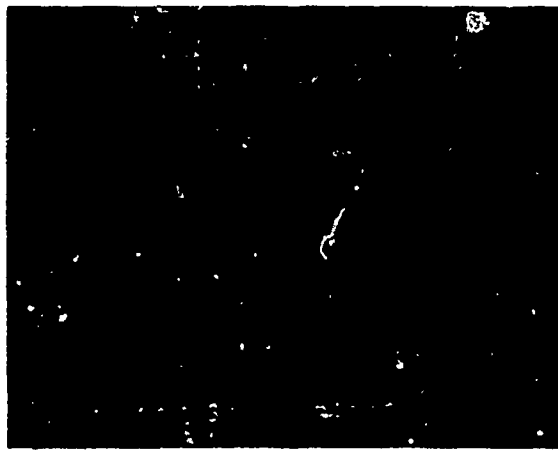
The paint shaker is of interest because it also has no bearings which can be penetrated by the mix, and because it agitates the material more vigorously than the TS. The machine we use is designed to hold a gallon can. We found that it would not mix AP/AI when we used the polysulfone beads to combat agglomeration. Seven golf balls with 500 g of mix also failed to produce a good mix (5 minutes running time). A good mix was obtained when 1000 g of AP25/AI5 and 500 g of the porcelain balls were shaken for 5 minutes, see Figure 5. The figure contains two views; the cylinder was rotated  $180^\circ$  for the view on the right. The cylinder is 38 mm in diameter and the largest agglomerate is about  $300\mu$  across. The average agglomerate has a dimension of about  $100\mu$ , with a few in the 500 to  $1000\mu$  range. This charge is also far better than that shown in Figure 3, and the blending time is reduced by a factor of 12. Figure 6 shows the results obtained when a kilogram of 90/10 AP7/AI5 was mixed with 500 g of the ceramic balls (mixing time was 5 minutes). Charge #1 was pressed at 30 kpsi while Charge #2 was pressed to 15 kpsi. The charges were ~100% and 96.7% TMD, respectively. Sizes of the spots (which are not visible in the photograph) are given in the caption of Figure 6. Both these charges are also superior to that shown in Figure 3. Hence, we have a method for handling the 25 $\mu$  AP and 7 $\mu$  AP. This method is convenient and very rapid. The only question about the method is its safety, the small size of the batch, and the necessity for screening to remove the porcelain balls.

We have also made a three-component model propellant consisting of AP, Carnauba wax and HMX. Photographs of the ends of charges made from a mix of AP25/Wax/HMX, 74/20/6 are shown in Figure 7. The TS was run for one hour and was loaded with 3.5 kg of the mix and four golf balls. Some idea of the size of the spots can be inferred by comparison with the inside diameter of the steel casing, 3.5 cm. Obviously more vigorous means are required to combat the tendency of 25 $\mu$  AP to agglomerate.

When 652 of the ceramic balls were loaded in the TS along with 1.0 kg of a mix of the components mentioned above (71/20/9) fairly good mixes were obtained. Photographs of the samples are shown in Figure 8a (side view) and Figure 8b (end view), and the samples are partially described in Table A1. Samples 3 and 4 are from the same batch; sample 3 was removed after 10 minutes of mixing after which

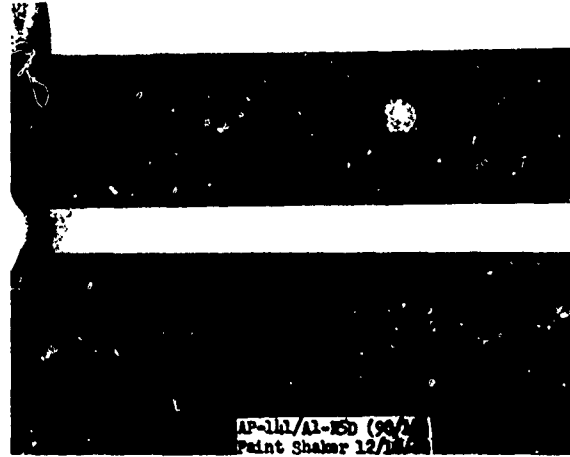


FIG. A4 AP( $\sim 7\mu$ )/Al( $\sim 5\mu$ ) (90/10) PREPARED IN THE TWIN SHELL BLENDER WITH CERAMIC BALLS.



→ 1 CM ←

FIG. A5 CHARGE PRESSED FROM 90/10 MIX OF  $25\mu$  AP/ $25\mu$  Al IN PAINT MIXER WITH PORCELAIN BALLS.



CHARGE #1  
LARGEST SPOT SIZE  $\sim 900\mu$   
AVERAGE SPOT SIZE BETWEEN 100 AND  $200\mu$

CHARGE #2  
LARGEST SPOT SIZE  $\sim 900\mu$   
AVERAGE SPOT SIZE BETWEEN 200 AND  $300\mu$

FIG. A6 CHARGE PRESSED FROM 90/10 MIX OF  $7\mu$  AP/ $5\mu$  Al IN PAINT MIXER WITH PORCELAIN BALLS.



FIG. A7 THREE COMPONENT PROPELLANT MODEL MIXED IN TWIN SHELL BLENDER WITH FOUR GOLF BALLS.

58

the blender was run for an additional 10 minutes to produce the material for sample 4. Samples 5 and 6 were made in a similar way; 5 being removed after 60 minutes, the remainder of the mix was treated for another 60 minutes to produce the material for sample 6. Sample 3 (10 minutes) is the worst of the four, see Figures 6a and 6b and Table A1. We judged the 20-minute mix, sample 4, to be the third best; its chief defect being one spot in the side view. It is interesting, and encouraging, that sample 5 was judged to be better than sample 6, i.e., that mixing for one hour gives a better sample than mixing for two hours. Sample 5 is the best of the four which once again indicates that we are not mixing in the conventional sense, but are combining a mixing and milling operation.

Table A1

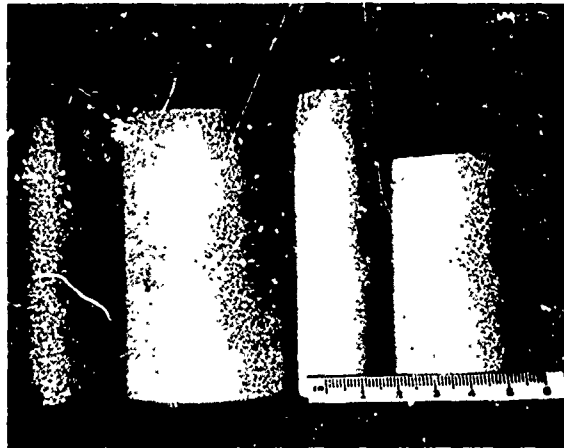
SAMPLES OF THE THREE COMPONENT MODEL PREPARED IN THE PATTERSON-KELLY TWIN SHELL BLENDER WITH CERAMIC BALLS FOR MILLING.

COMPOSITION: 25 $\mu$  AP/CARNAUBA WAX/14 $\mu$  HMX, 71/20/9

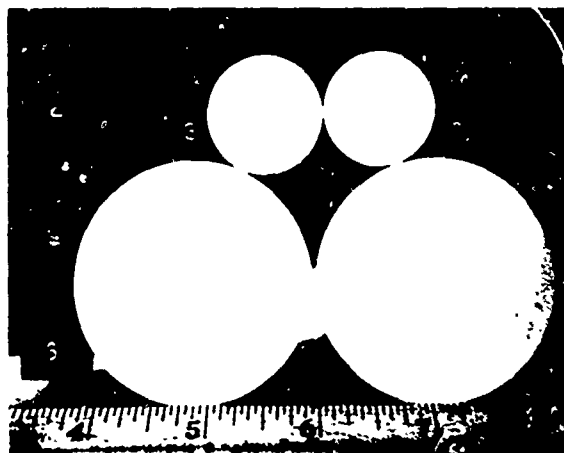
Sample Number	Mixing Time, Minutes	Largest Spot On Surface, $\mu$	Average Spot Size, $\mu$	Comments
3	10	2,300	100 - 600	Worst of four samples. Several spots between 1,000 and 2,000 $\mu$ across.
4	20	1,500	100 - 200	Third best of the four samples. Chief defect is one large spot on side.
5	60	200	<100	Fewest spots of the four samples. Rated best.
6	120	200	<100	Second best of the four samples.

In order to run a gap test (LSGT) of the three-component mix, six mixes of AP25/Wax/HMX, 70/20/10 were prepared. a compromise was made on the duration of mixing -- 30 minutes. Each batch contained 1.0 kg of the propellant model and about 600 ceramic balls. A 590 $\mu$  screen was used to separate the balls from the mixes, which were then blended for 30 minutes in a rotating barrel (about 14 gallon capacity). This mix was much better than that represented in Figure 7.

Mixers with Internal Agitators. It has been recognized for some time that good mixing could not be obtained in a conventional mixer such as the TS. A few golf balls have been used in this mixer to



a. SIDE VIEW



b. END VIEW

FIG. A8 THREE COMPONENT MIX PREPARED IN THE TWIN SHELL MIXER  
WITH CERAMIC BALLS.

60

provide some milling action. In order to determine the effects of more vigorous agitation and milling, we used a WB having a maximum capacity of one quart. Although the agitator speed is 11,000 r.p.m., or greater, in the WB, it would not mix sodium bicarbonate and Al5. The impeller produced a void which was bridged by the mix. In order to make the mix circulate, plastic (polysulfone) beads (rough cylinders, about 3 mm in both diameter and length) were added. The impeller threw these beads into the mix, overcoming the bridging and producing circulation.

Three batches of 90/10, AP7/Al5 were prepared in the WB using 165 g of mix and 116 g of the beads. The machine was run for 1 minute, after which it and the mix were examined. Because of the vigor of the agitation, the material was heated noticeably. After 5 minutes, the machine was run for another one-minute period. The pressed cylinders made from these mixes were examined as described above and photographed -- see Figure 2. There are very few agglomerates of AP visible in the photograph, or on the cylinders themselves. The largest spot has a dimension of about  $500\mu$ , the average being between 100 and  $200\mu$ . These charges are comparable to the best AP/Al charges we have prepared in the present work.

The overall length of the blades in the WB is 6.4 cm (2.5 in.). At 11,000 r.p.m. (under load, measured with a stroboscopic light), the tip speed is  $1.2 \times 10^5$  cm/min (7,200 ft/min). It is this high speed which produces the heating in the mix. Particle size measurement (micromerograph on AP7 before and after exposure in the WB) failed to show any change in particle size. No grinding of the plastic beads could be detected in other tests. We observed no trouble with the bearing which is a simple sleeve bearing. Concern may have been overemphasized about the hazard associated with the use of bearings into which a mix can penetrate. Our experience shows that the WB can be used to mix AP and aluminum and that it gives a very good mix. The quantity mixed at one time is small (165 g in our trials) but the batch frequency is relatively high -- say six batches per hour. This would be competitive with the twin shell mixer as we have been using it.

A blender having a capacity of one gallon (compared to one quart) is available. Such a machine would require less manpower for our mixing by increasing the rate of production. Most of our investigations require more product than can be produced in either WB.

The other machine which has internal agitators is the TSIB. The bar is really a rod which extends through the mixer, supported by bearings concentric with those which support the shell. The rod is equipped with agitators and is driven by a second electric motor. Tip speed in the eight-quart machine is 1,700 ft/min as compared with 7,200 ft/min in the small WB, so that the TSIB should be safer to use. Bearings should cause less trouble, due partly to the lower speed of the shaft, and partly to their locations on the sides of the shells. In the WB, the bearing is at the bottom of the vessel -- the worst possible location.

The TSIB presumably combines the good mixing action of the twin shell blender with some of the milling action of the WB. We borrowed a four-quart unit from the Naval Ordnance Station, Indian Head, Maryland. Because the machine was in poor condition, it was returned to the manufacturer, Patterson-Kelley, for reconditioning. The reconditioned blender was then used to produce 90/10 mixes of AP N-139 (average particle size less than  $10\mu$ ) and  $5\mu$  aluminum powder in 1 kg batches. The AP has been in storage for about two years so that it had formed into clumps. These were broken up and all material was forced through a  $590\mu$  screen. This operation, and the following weighing operation were performed in a dry nitrogen atmosphere to minimize moisture pickup. The constituents were mixed for 20 minutes after which the material was again forced through the  $590\mu$  screen (this was done in air). A charge pressed from this mix was very speckled, the largest spot being about  $400\mu$  in dimension, the average being about  $200\mu$ . This mix was not as good as was desired; it was concluded that the twin shell blender with intensifier bar was not giving the material the required milling action.

For the next mix, 500 g of polysulfone beads were added to the load. A very good charge resulted. Only six specks were observed on its surface; the largest spot was about  $200\mu$  across. This demonstrated that the twin shell blender could be used to produce the quality of mixes which we desired. The disadvantages are that the plastic beads must be added to the mix, and that the machine has bearings into which the mix can enter. The 20-minute interval required is tolerable.

Table A2 contains the charge preparation data for the two mixtures described above as well as three others made in studying the P-K blender. The additional results will be described in the next section.

#### Adopting a Method for Mixing AP/Al

For a time we mixed AP and aluminum in the paint shaker using ceramic balls as mentioned above. Several of the 1.0 kg batches were later blended in the rotating barrel blender. Because of the size of the batch, this latter operation was conducted in a remote location. Elimination of this operation would not only save manpower, it would also decrease our exposure to a possibly hazardous operation.

Five charges were prepared to determine if the detonation velocity was sensitive to the method in which the mix was prepared. Mixes for two of these charges were prepared in the paint shaker. Operations during and following mixing are denoted by the x's in the first column of Table A2. Note that the initial screening and the weighing was done in a dry nitrogen atmosphere. Final screening was done in air. The charge prepared from this material was speckled, the largest specks being about  $800\mu$  across. The average dimension of a speck was about  $200\mu$ . Another specimen was made, see Column 5 in Table A2. This time the material was not screened, and it was weighed in air. A  $250\mu$  screen was used for final screening

Table A2

OPERATIONS IN THE PREPARATION OF EXPERIMENTAL CHARGES OF  
AP N-139 AND ALUMINUM (90/10) AND RESULTS

MIX #	1	2	3	4	5
Screened (590 $\mu$ ) in N <sub>2</sub> prior to mixing	X	X	X		
Screened (590 $\mu$ ) in open air prior to mixing				X	
Weighed in N <sub>2</sub> (0.9 kg AP + 0.1 kg Al)	X	X	X		
Weighed in open air (0.9 kg AP + 0.1 kg Al)				X	X
Mixed in paint can shaker with 500 g ceramic beads for six minutes	X				X
Mixed in Twin Shell using Intensifier bar (20 minutes)		X			
Mixed in Twin Shell using Intensifier bar with 500 g polysulfone beads (20 minutes)			X	X	
Screened (590 $\mu$ ) in open air prior to pressing	X	X	X	X	
Screened (250 $\mu$ ) in open air prior to pressing					X
Pressed isostatically and machined to 1-3/8" diam x 9"	X	X	X	X	X
Density of charge (g/cc)	1.325	1.318	1.331	1.318	1.310
Ranking by quality <sup>1</sup>	5	4	1	2	3
Detonation velocity (mm/ $\mu$ sec) <sup>2</sup>	4.375	4.335	4.451	4.388	4.375
Detonation velocity (corrected to 1.32 g/cc) <sup>3</sup>	4.363	4.340	4.426	4.391	4.398

<sup>1</sup>Quality was determined by visual examination using a 12X magnifier.

Quality of mix judged to be as follows:

1st Mix 3 - Fewest specks (only six observed), largest 200 $\mu$ , average size 100-150 $\mu$

2nd Mix 4 - Extremely few specks (very close 2nd to mix 3), largest speck 500 $\mu$

3rd Mix 5 - A lot more speckled than Mix 3 and 4 but less speckled than Mixes 1 and 2, largest speck 500 $\mu$ , average size 100-150 $\mu$

4th Mix 2 - Very speckled, largest 400 $\mu$ , average 200 $\mu$

5th Mix 1 - Most speckled, largest 800 $\mu$ , average 200 $\mu$

<sup>2</sup>Shot Nos. 854 - 858.

<sup>3</sup>The corrected detonation velocity was obtained by using

$\Delta D = b (\rho_2 - \rho_1)$  where  $b$  is the slope of the  $D$  vs  $\rho$  line for 1-3/8" diameter charges of AP N-141/Al H5D (90/10), and  $\rho_1$  is the average density, 1.32 g/cc.,  $b = 2.3$ . Detonation velocity data for AP N-141 is given in Table A3; those for the 90/10 mixture are in Table 3 of the text.



Table A3

DETONATION VELOCITY DATA FROM FINE APs AT  $d = 50.8$  mm

Shot No.	$\rho_o$ g/cc	D mm/ $\mu$ sec
<u>AP N-139</u>		
672	1.006H	3.466
673	1.006H	3.508
<u>AP N-141</u>		
878	0.801H	2.900
877	1.001H	3.494
872	1.181i	3.965
873	1.223i	4.053
874	1.303i	4.195
875	1.421i	4.306
876	1.478i	4.058

64

and to recover the ceramic balls. The perversity of this material is illustrated by the fact that the charge had a speck as large as  $500\mu$  across even though the mix had passed through a  $250\mu$  screen. The average size of the specks was in the range of 100 to  $150\mu$ . Hence, a good mix was obtained from substandard material (lumped AP) which was handled in air.

Three more charges were prepared using the TSIB. Two of these were described in the preceding section. See Columns 2 and 3 for the schedule of operations involved. A third mix was prepared by screening and weighing in air, see Column 4. The rank in quality of these three charges, and the two prepared from mixes from the paint shaker are given near the bottom of Table A2. Note that those from mixes 3 and 4 are both very good -- operating in the open air of the mixing room has no serious deleterious effect on the appearance of the charges. Mix No. 2 gave a charge covered with small specks indicating that the milling action of the polysulfone beads is more important than is the dry, nitrogen atmosphere.

The densities of the five charges discussed above are also given in Table A2 as well as the measured detonation velocities. These detonation velocities have been adjusted to a density of  $1.32 \text{ g/cc}$  by using the slope of the  $D$  vs  $\rho$  curve for the same diameter charges of AP N-141, a slightly finer material. These normalized velocities are given in the last line of Table A2. The average of these velocities is  $4.384 \text{ mm}/\mu\text{sec}$  so the greatest deviation is 0.044 or about 1.0%. This indicates that the mixing procedures are barely distinguishable as far as the detonation velocity measurements are concerned. This is encouraging because it should be possible to obtain good results with frequently prepared small batches rather than having to make many small batches at one time and blend them in the rotating barrel. The mixes prepared in the TSIB with the plastic beads to break up agglomerates gave the greatest normalized detonation velocities, which may indicate that they were actually better mixtures, as was indicated by the more subjective visual examinations. The paint shaker method is the more convenient to use and is safer insofar that there are no bearings in which the mix can become caught and heated. For these reasons, the paint shaker method is the preferred one.

## Appendix B

INFORMATION ON  $D = D(\Delta, u)$  FOR ALUMINIZED ORGANIC H.E.

## HBX-1

The pattern of  $D = D(\Delta, u)$  for HBX-1 (RDX/TNT/Al/Wax, 40/38/17/5) was used as an example of Group 1 behavior in reference 4. Subsequently Roslund & Coleburn published the data<sup>6</sup> from which that pattern had been constructed. However, since they did not tabulate some of the results of interest here, the coefficients of the straight lines fitted by least squares to the data were obtained from reference 7 and listed in Table B1. The small difference between the ideal value  $D_i$  in Table B1 from reference 7 and that given in reference 6 was caused by a revision of the latter data after a recalibration of the camera used. The revised data differ slightly in absolute value, but would show the same trends. The important point to establish here is the linear relationships between the coefficients  $a(u)$  and  $b(u)$  and the reciprocal diameter  $u$ . The equations are given at the bottom of Table B1 and the curves are shown in Figure B1. They extend only up to  $u = 0.079 \text{ mm}^{-1}$  ( $d = 12.7 \text{ mm}$ ), because the data obtained at  $d = 6.4 \text{ mm}$  diverge so far from the trends that they are off-scale in Figure B1. Such divergence would be expected as the material approaches its critical condition, and this is approached at any  $\Delta$  as the diameter is decreased.

The relationships of Table B1 and Figure B1 lead to the general expression for this pressed HBX-1 of

$$D(\Delta, u) = 0.16 - 37.01u + (7.34 + 38.32u)\Delta \quad (\text{B1})$$

Equation (B1) leads to the fan of curves illustrated in references 4 and 6 with straight lines coalescing at  $\Delta = 0.97$  and having slopes which increase with increasing  $u$ .

## Tritonal 67.8/32.2

TNT/Al, 67.8/32.2 is the nominally stoichiometric mixture. It has been studied for diameter effect on  $D$  and the revised data<sup>7</sup> are listed in Table B2; the value of the coefficients  $a(u)$ ,  $b(u)$ , obtained by least square fits are also given. As in the case of HBX-1, these coefficients are linear functions of  $u$ ; this is illustrated in Figure B2 and their equations are presented at the bottom of Table B2. The general equation for this mix of tritonal 67.8/32.2 is:

66

NOLTR 72-15

$$D(\Delta, u) = -1.53 - 16.69u + (8.685 + 14.92u)\Delta \quad (B2)$$

This is again the Group 1 pattern and is illustrated in Figure 10 of the text.

Table B1

LEAST SQUARE FITS TO HBX-1 DATA<sup>6,7</sup> IN  
FORM  $D(\text{mm}/\mu\text{sec}) = a(u) + b(u)\Delta$

$d(\text{mm})$	$u(\text{mm}^{-1})$	$a(u)$	$b(u)$
$\infty$	0	0.169	7.334
50.8	0.01969	$-0.403 \pm 0.133$	$7.925 \pm 0.146$
25.4	0.03937	$-1.595 \pm 0.111$	$9.104 \pm 0.123$
12.7	0.07874	$-2.740 \pm 0.197$	$10.287 \pm 0.213$
6.35	0.1570	$-19.79 \pm 0.073$	$27.650 \pm 0.074$

Curves of Figure B1

$$a(u) = 0.16 - 37.01u$$

$$b(u) = 7.34 + 38.32u$$

$$\rho_v = 1.76 \text{ g/cc}$$

68

NOLTR 72-15

Table B2

DETONATION VELOCITY DATA FOR TNT/Al, 67.8/32.2  
 $\rho_v = 1.89 \text{ g/cc}$

Least Square Values for  $D = a + b\Delta$

d(mm)	$\rho_0 \text{ g/cc}$	$\Delta$	D(mm/ $\mu\text{sec}$ )	u(mm $^{-1}$ )	a(u)	b(u)
12.7	1.15	0.608	3.165			
12.7	1.37	0.725	4.260			
12.7	1.57	0.831	5.330			
12.7	1.82	0.963	6.650			
				0.07874	-2.858	9.860
25.4	1.14	0.603	3.400			
25.4	1.19	0.630	3.590			
25.4	1.33	0.704	4.320			
25.4	1.33	0.704	4.330			
25.4	1.34	0.709	4.440			
25.4	1.35	0.714	4.565			
25.4	1.43	0.757	4.940			
25.4	1.52	0.804	5.320			
25.4	1.62	0.857	5.850			
25.4	1.72	0.910	6.260			
25.4	1.80	0.952	6.660			
25.4	1.81	0.958	6.625			
				0.03937	-1.158	9.266
50.8	1.14	0.603	3.560			
50.8	1.46	0.772	5.035			
50.8	1.72	0.910	6.320			
				0.01969	-1.873	8.984
$a(u) = -1.53 - 16.69u$ $b(u) = 8.685 + 14.92u$						

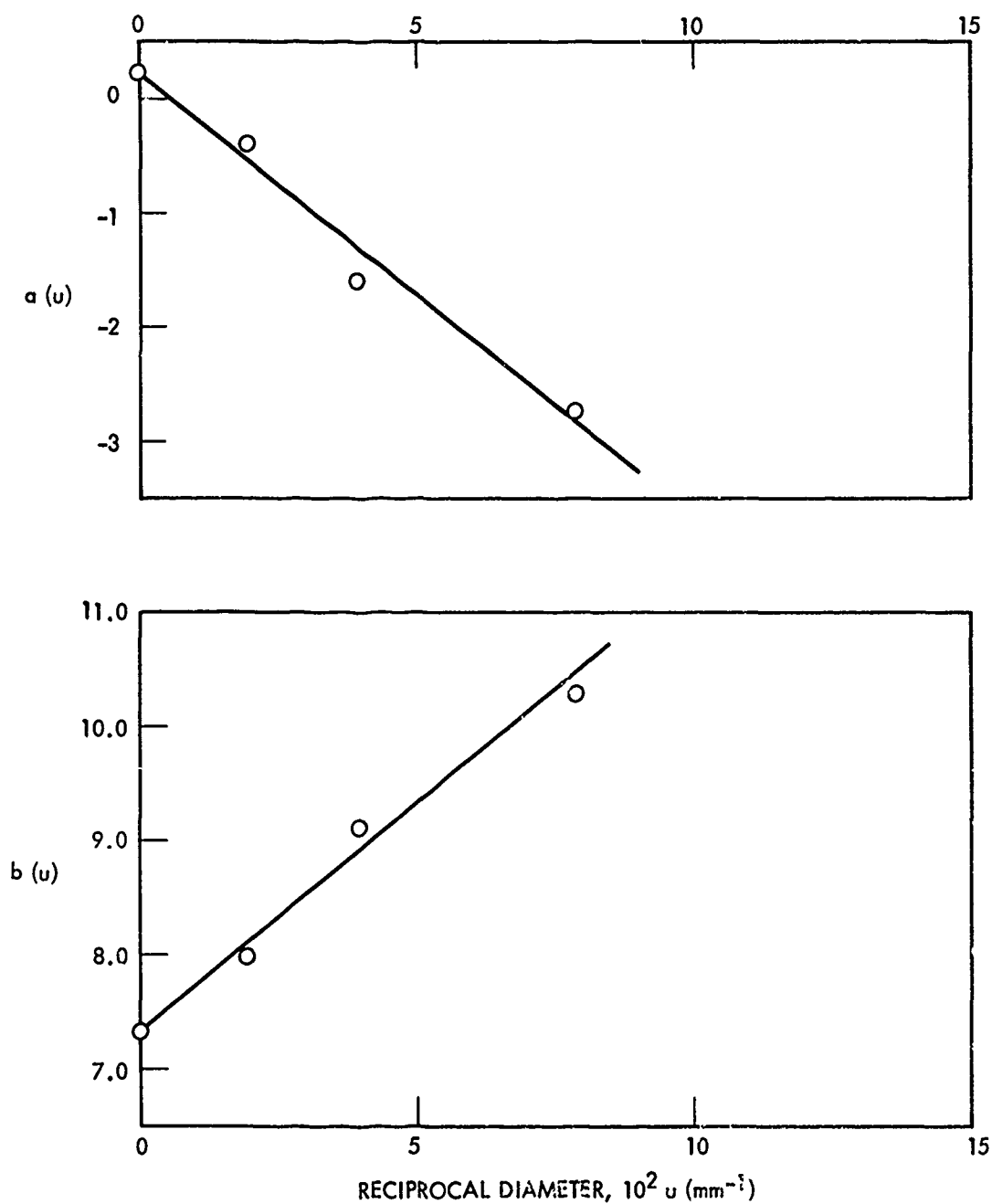


FIG. B1 VARIATION OF COEFFICIENTS  $a(u)$ ,  $b(u)$  FOR HBX-1

70

NOLTR 72-15

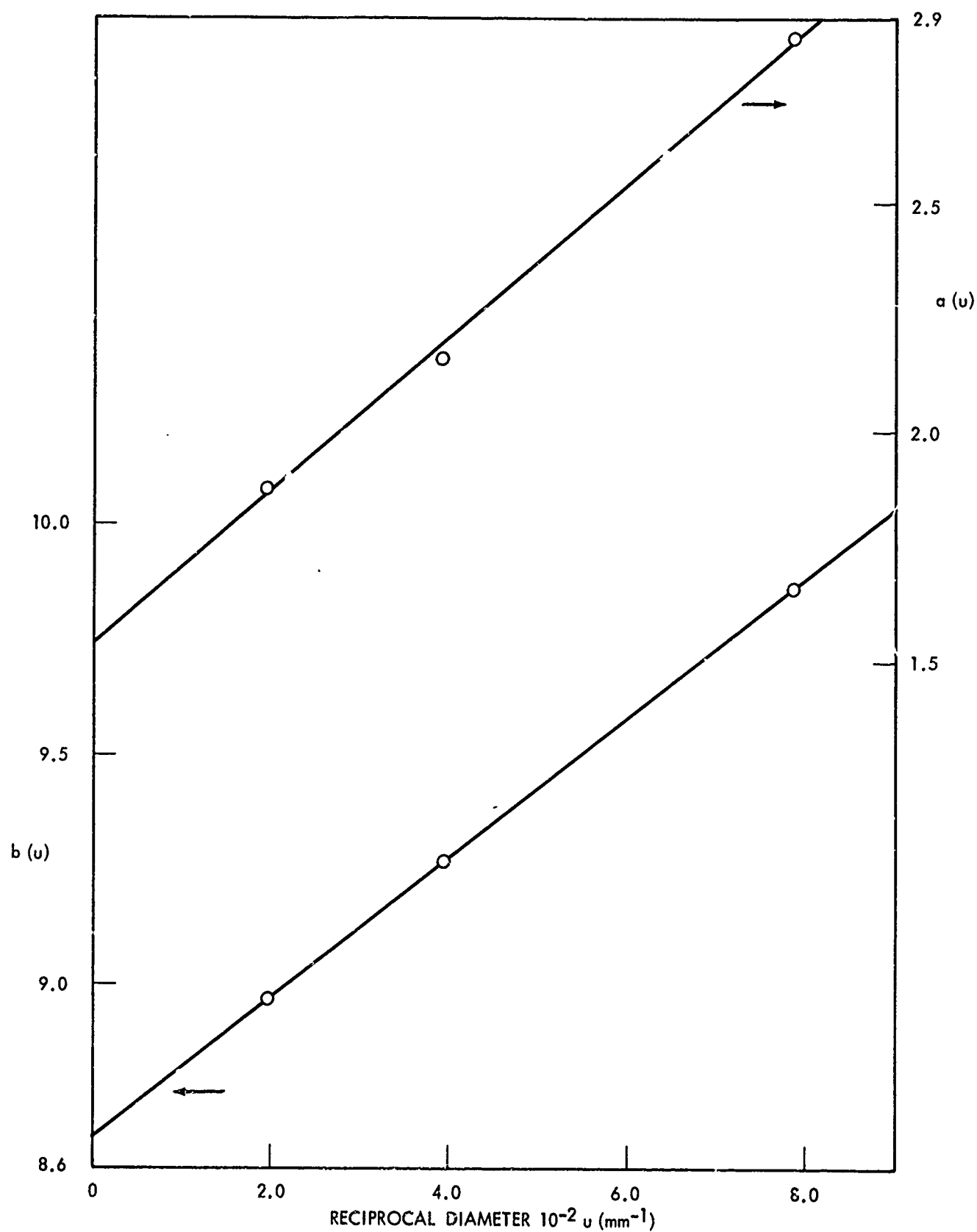


FIG. B2 VARIATION OF COEFFICIENTS  $a(u)$ ,  $b(u)$  FOR TRITONAL 67.8/32.2



## Appendix C

## ALUMINIZED ORGANIC H.E. AT CONSTANT DIAMETER

Three simple binary mixtures of aluminum with an organic H.E. were used at a fixed diameter ( $d = 50.8$  mm) to determine the effect of Al concentration on the measured detonation velocity. The D- $\Delta$  data were in each case fitted to a straight line by the method of least squares.<sup>7</sup> The resultant coefficients are given in Table C1.

In the case of RDX and TNETB, a 51 mm diameter seems large enough for the non-aluminized explosive to exhibit its ideal detonation velocity. Hence, literature values are used for these two H.E. TNT, however, may still show a significant diameter effect at  $d = 51$  mm; the situation is further complicated by a reported departure of its D- $\Delta$  curve from linearity at high density.<sup>8</sup> For both reasons, the rate chosen for TNT was that obtained by extrapolating to zero the curves of  $a(u)$  vs %Al &  $b(u)$  vs %Al.

As Figure C-1 shows, both coefficients of the D- $\Delta$  curve are smooth functions of the aluminum content of the mixture. In the case of TNETB, the curves appear linear; this was assumed to be the case also in extrapolating the TNT curves. The RDX curves are practically linear 10% to 30% Al, but both the lower and higher Al contents show that the  $a(u)$  curve is concave upward; the  $b(u)$ , convex upward.

All data at concentrations above 32% Al have been omitted from Figure C-1. In the case of the TNT series there appeared to be a discontinuity above this concentration in the  $b(u)$  curve. For the RDX and TNETB series, there is no apparent discontinuity. But other treatments have shown that the data from higher Al content mixtures do not seem strictly comparable to those from less aluminized mixtures. This effect is certainly to be expected since we are considering rates at a fixed diameter of 51 mm instead of infinite diameter rates. At  $d = 51$ , the higher the Al content, the greater will be the difference between the rate measured and  $D_i$ .

Note that there is a small difference between the coefficients listed for TNT/Al, 67.8/32.2, in Table C1 and those derived from Equation B2 in the preceding appendix. This occurs because the data used in Appendix B has been revised, whereas those of Table C1 have not.

72

Table C1

EFFECT OF ALUMINUM ON DETONATION RATE OF THREE  
EXPLOSIVES (d = 5.08 cm)

Wt Fraction of Al x	Voidless Density $\rho_v$	Coefficients Eq (4) for d = 5.08 cm		Al/O*	k*
	g/cc	a	b		
<u>TNT/Al</u>					
0	1.65	2.300	4.754 <sup>1</sup>	0	1.4306
0.106	1.72	0.948	6.106	0.170	
0.217	1.80	-0.344	7.398	0.398	
0.322	1.89	-1.772	8.826	0.680	
<u>RDX/Al</u>					
0	1.802	2.515	6.246 ref 9	0	1.3727
0.10	1.86	0.100	8.742	0.153	
0.20	1.93	-1.600	10.422	0.343	
0.30	2.00	-3.100	12.000	0.588	
0.40	2.08	-4.592	13.312	0.915	
0.50	2.16	-6.078	14.688	1.371	
<u>TNETB/Al</u>					
0	1.78	1.947	6.515 ref 10	0	1.024
0.10	1.84	0.820	7.691	0.114	
0.20	1.91	-0.200	8.404	0.256	
0.30	1.98	-1.200	9.504	0.438	
0.50	2.15	-4.038	12.148	1.022	

<sup>1</sup>By extrapolation; see Figure C-1

\*Al/O = k x/(1-x)

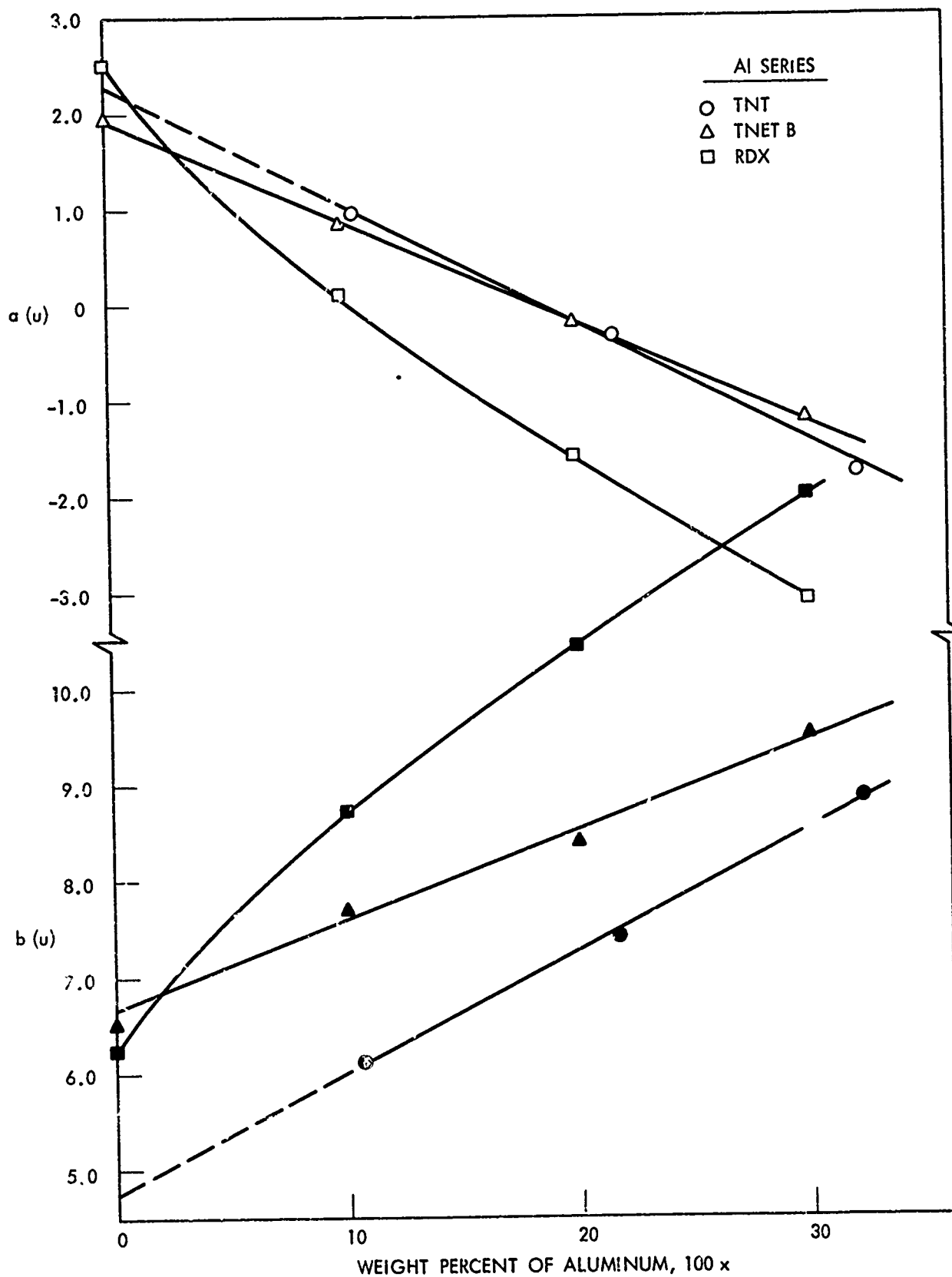


FIG. C-1 VARIATION OF COEFFICIENTS  $\alpha$ ,  $b$  WITH ALUMINUM CONCENTRATION